AGU PUBLICATIONS

Reviews of Geophysics

REVIEW ARTICLE
10.1002/2014RG000451

Key Points:
- Bars and subaqueous levees form at river mouths
- River mouth deposits can be used to build new land
- Waves, tides, and vegetation affect river mouth deposits

Correspondence to:
S. Fagherazzi,
sergio@bu.edu

Citation:
Fagherazzi, S., D. A. Edmonds, W. Nardin, N. Leonardi, A. Canestrelli, F. Falcini, D. J. Jerolmack, G. Mariotti, J. C. Rowland, and R. L. Slingerland (2015), Dynamics of river mouth deposits, *Rev. Geophys.*, *53*, doi:10.1002/2014RG000451.

Received 11 MAR 2014
Accepted 21 MAY 2015
Accepted article online 26 MAY 2015

Dynamics of river mouth deposits

Sergio Fagherazzi[1], Douglas A. Edmonds[2], William Nardin[1,2], Nicoletta Leonardi[1], Alberto Canestrelli[3], Federico Falcini[4], Douglas J. Jerolmack[5], Giulio Mariotti[6], Joel C. Rowland[7], and Rudy L. Slingerland[3]

[1]Department of Earth and Environment, Boston University, Boston, Massachusetts, USA, [2]Department of Geological Sciences, Indiana University, Bloomington, Indiana, USA, [3]Department of Geosciences, Pennsylvania State University, State College, Pennsylvania, USA, [4]Istituto di Scienze dell' Atmosfera e del Clima, Consiglio Nazionale delle Ricerche, Rome, Italy, [5]Department of Earth and Environmental Science, University of Pennsylvania, Philadelphia, Pennsylvania, USA, [6]Department of Earth, Atmospheric and Planetary Sciences, Massachusetts Institute of Technology, Cambridge, Massachusetts, USA, [7]Earth and Environmental Sciences Division, Los Alamos National Laboratory, Los Alamos, New Mexico, USA

Abstract Bars and subaqueous levees often form at river mouths due to high sediment availability. Once these deposits emerge and develop into islands, they become important elements of the coastal landscape, hosting rich ecosystems. Sea level rise and sediment starvation are jeopardizing these landforms, motivating a thorough analysis of the mechanisms responsible for their formation and evolution. Here we present recent studies on the dynamics of mouth bars and subaqueous levees. The review encompasses both hydrodynamic and morphological results. We first analyze the hydrodynamics of the water jet exiting a river mouth. We then show how this dynamics coupled to sediment transport leads to the formation of mouth bars and levees. Specifically, we discuss the role of sediment eddy diffusivity and potential vorticity on sediment redistribution and related deposits. The effect of waves, tides, sediment characteristics, and vegetation on river mouth deposits is included in our analysis, thus accounting for the inherent complexity of the coastal environment where these landforms are common. Based on the results presented herein, we discuss in detail how river mouth deposits can be used to build new land or restore deltaic shorelines threatened by erosion.

1. Introduction

The area in front of the mouth of deltaic distributary channels and rivers is a location where sediments accumulate and new land forms. At these locations sediment deposition can occur by growth of natural levees and channel elongation or by deposition and vertical aggradation of mouth bars (Figure 1). Irrespective of their shape and evolution, these landforms are of paramount importance within the coastal landscape because, after emerging, they become deltaic islands and subaerial levees, which protect coastal communities [*Costanza et al.*, 2008] and provide habitat for rich and productive ecosystems [*Gosselink and Pendleton*, 1984]. In general, land naturally builds and erodes in relation to switching depocenters of rivers debouching in the ocean and sea level oscillations over long timescales, and storms and river floods over shorter timescales. In recent decades several river mouth landforms have been deteriorating because of sediment starvation triggered by the damming of large rivers, which reduces the flux of sediments to the ocean [*Syvitski et al.*, 2005]. In a period in which sea level rise is enhancing coastal erosion and flooding [*Nicholls and Mimura*, 1998], it is more important than ever to understand the physics of river mouth sediment deposits and how new land is built. In fact, deposition of sediments at river mouths not only can mitigate coastal erosion but it can also promote land expansion thus restoring anthropogenically modified coastlines [*Paola et al.*, 2011; *Nittrouer et al.*, 2012a; *Edmonds*, 2012, *Kim et al.*, 2009b; *Kim*, 2012].

Here we limit our analysis to areas close to river and distributary channel mouths, up to few kilometers, and to time scales from yearly events to decades. Sand deposits are the main focus of this review, since they preferentially form near river mouths given the high settling velocity of sand. Consequently, we do not cover the dispersal of fine sediment on the shelf and the large-scale dynamics of riverine buoyant plumes [e.g., *Horner-Devine*, 2009]. The results presented here are valid in shallow water (up to few meters), where stratification effects are limited and the river flow can be represented by a bounded, planar turbulent jet. Furthermore, we do not consider secondary flow circulations.

Wright [1977] provides an excellent review of research results on sediment transport and deposition at river mouths. He suggests that effluent behavior and depositional patterns are affected by outflow inertia, bed

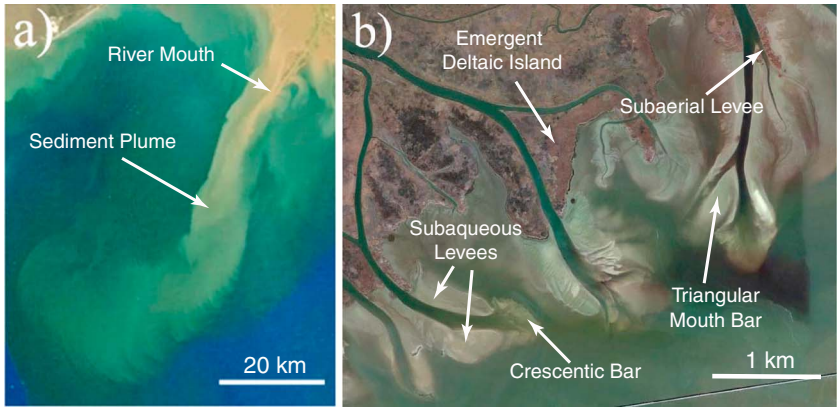

Figure 1. (a) Sediment-laden plume in northern Gulf of Mexico from the Southwest Pass of the Mississippi Birdsfoot [from *Falcini and Jerolmack*, 2010]. (b) River mouth deposits in the Apalachicola Delta, Florida (imagery date 2 January 2012 courtesy of Google Earth).

friction, and buoyancy. Distinct deposits spring from the dominance of one of these forces. Inertial conditions reflect an unbounded jet debouching into a deep (relative to the river channel) basin that results in lunate bars or a classic "Gilbert-type" delta. In friction-dominated flows river mouth hydrodynamics are characterized by bed friction, rapid spreading, and rapid levee divergence around a central mouth bar. In contrast, channels with straight parallel banks, low width-to-depth ratios and infrequent bifurcations were attributed to river mouth settings characterized by buoyant or hypopycnal outflows. Moreover, *Wright* [1977] highlights the role of tides and waves in sediment dispersal and accumulation patterns. However, while capturing the main dynamics of sediment dispersal at river mouths and related deposits, the results reported in *Wright* [1977] are mostly qualitative in nature. This manuscript builds upon these early review by adding recent process-based results obtained through numerical modeling, detailed lab experiments, and novel theoretical approaches.

In recent years, numerical models based on the solution of fluid and sediment transport equations have helped unravel how flow hydrodynamics affect the formation of sediment deposits near river mouths, shedding light on the long-term development of deltas [e.g., *Overeem et al*., 2005; *Fagherazzi and Overeem*, 2007]. Numerical models have also allowed for scientists to test the validity of theory by simplified analytical approaches for river mouth morphodynamics. Among these the coupled hydrodynamic-sediment transport model Delft3D [*Roelvink and Van Banning*, 1994; *Lesser et al*., 2004] is becoming an increasingly common tool in morphodynamic studies, due to its numerical stability and ease of use compared to other platforms. Several of the numerical results presented in this review were obtained with Delft3D simulations.

Moreover, new techniques are available to measure flow dynamics, turbulence, and sediment transport in laboratory settings (e.g., acoustic Doppler velocimeters) [see *Rowland et al*., 2009a]. These new techniques are unraveling the complex relationships between the water jet exiting an orifice and sediment transport.

Detailed field measurements of both mouth bar sedimentology [e.g., *Esposito et al*., 2013] and sediment plumes exiting river mouths [e.g., *Falcini et al*., 2012] are providing new insights on sediment dynamics at river mouths. Finally, a revisitation of jet theory with the novel approach of sediment potential vorticity [*Falcini and Jerolmack*, 2010] allows us to better explain numerical and experimental results.

A full discussion based on the long-term evolution of deltaic landforms is beyond the scope of this review. The readers can refer to recent publications on the morphodynamic evolution of deltas [*Overeem et al*., 2005; *Fagherazzi and Overeem*, 2007; *Geleynse et al*., 2011; *Ashton and Giosan*, 2011, *Canestrelli et al*., 2014]. Similarly, we do not include herein the complex mechanism of river avulsion and how avulsions dictate delta progadation and morphology [*Slingerland and Smith*, 2004; *Jerolmack and Paola*, 2007; *Edmonds et al*., 2009; *Chatanantavet et al*., 2012]. Given the focus on mouth deposits, in this review we do not cover fluid mud and wave-driven gravity flows that transport sediments on the shelf in front of rivers [e.g., *Wright and Friedrichs*, 2006].

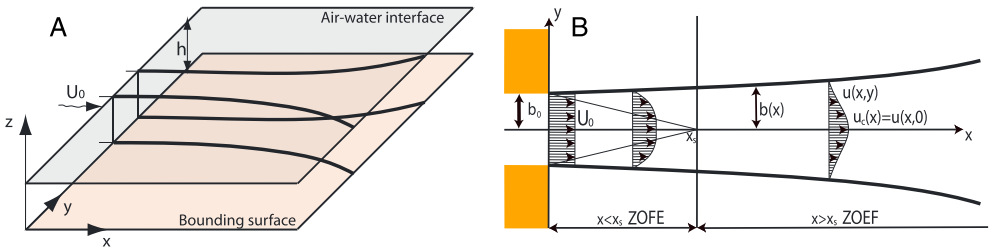

Figure 2. (a) Sketch of a planar bounded jet [from *Canestrelli et al.*, 2014]. (b) Sketch displaying the Zone of Flow Establishment (ZOFE) and the Zone of Established Flow (ZOEF). U_0 is the uniform velocity at the river mouth, b_0 is the jet half width, x_s is the distance at which the flow becomes established, and $u_c(x)$ is the jet velocity at the centerline [from *Nardin et al.*, 2013].

2. Hydrodynamics of Bounded and Unbounded Jets

In this section we describe the dynamics of river jets, restricting our discussion to exclude the effect of wind waves and tides, as well as any stratification due to gradients of temperature or salinity. Therefore, we present a case where a river debouches into a quiescent water body that has the same density of the incoming river fluid. The hydrodynamics at such a river mouth can be represented by a bounded plane turbulent jet, also called a "shallow" jet (Figure 2), Historically, most laboratory investigations on the hydrodynamic characteristics of plane jets were of the unbounded type; i.e., the bounding walls in Figure 2 were located as far as possible from the outlet in order to minimize their effect and establish a so-called "free" turbulent shear flow. Moreover, measurements were taken close to the orifice, i.e., for $x/h < 1$, where x is distance along the jet axis and h is the distance between the two bounding surfaces [e.g., *Bradbury*, 1965; *Goldschmidt and Young*, 1975; *Everitt and Robins*, 1978; *Ramaprian and Chandrasekhara*, 1985, among others]. On the contrary, when a plane jet is bounded, we have a so-called "shallow jet," in which the flow is characterized by an interaction between free turbulence and wall shear turbulence [*Jirka*, 1994]. Schematically, a turbulent jet can be divided in two well-defined zones (Figure 2b): (1) the zone of flow establishment (ZOFE), close to the inlet, in which the centerline velocity can be assumed constant and the flow quickly dissipates momentum, and (2) the zone of established flow (ZOEF), far away from the inlet, where a similarity velocity profile develops [*Ozsoy and Unluata*, 1982]. The ZOEF begins at the location at which the turbulence generated by shearing at the jet margins affects the entire jet [*Bates* 1953]. Indicating with $\xi = x/b_0$ the dimensionless along-axis coordinate, where b_0 is the half width of the outlet (i.e., the river mouth), we see that for a plane unbounded jet the transition between ZOFE and ZOEF occurs at a distance from the outlet $\xi_s = x_s/b_0$ between 4 and 6 [*Albertson et al.*, 1950; *Tennekes and Lumley*, 1972]. For a shallow (i.e., bounded) jet, *Rowland et al.* [2009a] reported a value of x_s/b_0 between 16 and 18 at the location where the transition between ZOFE and ZOEF occurs in their laboratory experiments. *Rowland et al.* [2009a] argue that this higher value might be related to their particular experimental setup at the mouth, since a pair of levees providing partial confinement were present, extending for 1 m into the basin. The presence of levees had likely reduced momentum dissipation, ultimately increasing the size of the ZOFE.

Experiments show that a self-preserving condition develops for unbounded jets in the ZOEF [*Kundu et al.*, 2011]. This allows the derivation of a similarity solution in which the lateral distribution of streamwise velocity is described by a normal distribution:

$$\frac{u(\eta)}{u_c} = \exp\left(-\frac{\eta^2}{2}\right), \tag{1}$$

where $u(\eta)$ is the velocity at any location $\eta = y/b(x)$ perpendicular to jet centerline, $b(x)$ is the local half width of the expanding jet, and u_c is the centerline velocity (the definition of all variables is also reported in the nomenclature table). Theory predicts that the centerline velocity in a plane jet decays at a rate $\propto x^{-1/2}$, while the increase of half-width $b(x)$ with x (also called jet spreading) is linear [*Kundu et al.*, 2011].

For bounded jets, shallow water theory predicts that bed friction causes a more rapid (i.e., exponential) jet spreading and deceleration with respect to an unbounded jet [*Borichansky and Mikhailov*, 1966; *Ozsoy*, 1977; *Ozsoy and Unluata*, 1982]. While the theory of *Borichansky and Mikhailov* [1966] neglects the

effect of water entrainment in the jet, this term is included in *Ozsoy* [1977] and *Ozsoy and Unluata* [1982]. The expressions for the dimensionless velocity $\overline{u} = u/U_0$ at the centerline of the jet, where U_0 is the velocity at the inlet, and the dimensionless width of the jet $\overline{b} = b/b_0$ for a horizontal bed read [*Ozsoy*, 1977]:

$$\overline{u} = \frac{e^{-\frac{S}{2}\xi}}{\left[e^{-S\xi_s} + \frac{4\alpha I_2}{SI_1}\left(e^{-\frac{S}{2}\xi_s} - e^{-\frac{S}{2}\xi}\right)\right]^{0.5}} \text{ and} \tag{2}$$

$$\overline{b} = \frac{e^{\frac{S}{2}\xi}}{I_2}\left[e^{-S\xi_s} + \frac{4\alpha I_2}{SI_1}\left(e^{-\frac{S}{2}\xi_s} - e^{-\frac{S}{2}\xi}\right)\right], \tag{3}$$

where $S = c_f B_0/(4h)$, with B_0, h, and c_f the mouth width, the water depth, and the friction factor, respectively. The entrainment rate (taken equal to 0.05) is α. I_1 and I_2 vary with ξ in the ZOFE, while they are constant in the ZOEF ($I_1 = 0.450$ and $I_2 = 0.316$). For a linearly sloping bed, it is still possible to obtain an analytical solution, while for a general bed configuration an ODE has to be solved numerically (for further details, see *Ozsoy and Unluata* [1982]). Note that friction reduces the longitudinal extension of the ZOFE compared to a classical plane jet configuration; therefore, as a first approximation, the main characteristics of the jet can be inferred by considering the ZOEF only [*Ozsoy*, 1977; *Nardin et al.*, 2013]. In this case the equations read

$$\overline{u} = \frac{e^{-\frac{S}{2}\xi}}{\left[1 + \frac{4\alpha I_2}{SI_1}\left(1 - e^{-\frac{S}{2}\xi}\right)\right]^{0.5}} \text{ and} \tag{4}$$

$$\overline{b} = \frac{e^{\frac{S}{2}\xi}}{I_2}\left[1 + \frac{4\alpha I_2}{SI_1}\left(1 - e^{-\frac{S}{2}\xi}\right)\right]. \tag{5}$$

Until the work of *Rowland et al.* [2009a], these shallow water theories were based on self-similarity velocity profiles without any validation coming from field or experimental data. In a series of laboratory experiments with shallow wall-bounded plane jets, *Rowland et al.* [2009a] found that for $x/B_0 > 9$ the mean velocity structure, streamwise velocity decay, spreading rate, and turbulence intensity agree well with existing plane jet theory. However, while the magnitudes and distribution of the cross-stream velocity, lateral shear stress, and lateral diffusivity of momentum were found in agreement with results for an unbounded plane jet, in proximity to the bed the three latter quantities deviated from those of a self-similar jet [*Rowland et al.*, 2009a]. In particular, lateral shear stresses and lateral diffusivity of momentum was an order of magnitude smaller close to the bottom than at the surface [*Rowland et al.*, 2009a]. These vertical variations suggest that to more accurately model delivery of suspended sediment to the jet margins, a three-dimensional numerical approach would be preferred because it will resolve diffusion in the lower part of the water column, where the largest concentration of suspended matter is located [*Rowland et al.*, 2009a]. Unfortunately, these dynamics cannot be captured by quasi 3-D models like Delft3D, which are based on the hydrostatic assumption along the vertical coordinate.

For $x/h > 10$, *Dracos et al.* [1992] experiments show that the jet begins meandering, and it is flanked by two sets of counter-rotating vortices. The confining effect of the bed is clearly seen in the turbulence spectrum of the jet: while in planar jets the spectrum at small wave numbers follows the three-dimensional cascading turbulent flow law with a $-5/3$ wave number dependence [*Goldschmidt and Young*, 1975], in bounded jet this cascade occurs only close to the mouth ($x/h < 10$), while in the far field the energy transfer at small wave numbers follows a -3 wave number dependence [*Dracos et al.*, 1992; *Rowland et al.*, 2009a; *Landel et al.*, 2012] typical of quasi-two-dimensional turbulence [*Batchelor*, 1969]. In the far field of bounded jets and for large wave numbers, the classical 5/3 law is recovered, a direct consequence of three-dimensional turbulence generated at the bed. The break in slope of the energy spectrum separates the two regions in which each process is dominant [*Rowland et al.*, 2009a].

Moreover, an inverse cascade of energy occurs, whereby energy is transferred from the inertial subrange to smaller wave numbers (i.e., to the larger counter-rotating vortices). *Dracos et al.* [1992] indicate that the secondary currents and the meandering pattern of the jet do not significantly affect the decay of the centerline velocity and jet spreading. A scale analysis [*Canestrelli et al.*, 2014] indicates that in order to properly capture the large coherent structures of the flow, the hydrostatic approximation can be safely employed. This approximation might fail for small local turbulent eddies, such as the secondary circulation

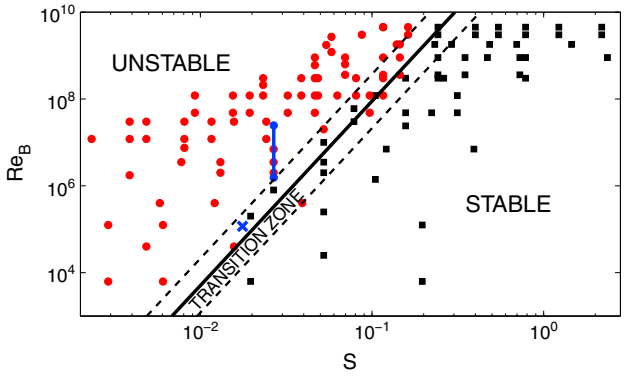

Figure 3. Stability diagram for a shallow jet ($B_0 \geq h$) debouching in quiescent waters [from *Canestrelli et al.*, 2014]. The red circles indicate unstable (i.e., meandering) jets; the black squares indicate stable jets, without large-scale horizontal coherent structures. The continuous and dotted lines represent equations (8)–(10), respectively. The cross represents the experimental data from *Rowland et al.* [2009a], while the blue line ending with blue circles represents the data of the tie channels in the Fly River system (Papua New Guinea) as presented in *Day et al.* [2008].

caused by bed friction and detected in experiments that produce very narrow bounded jets [e.g., *Foss and Jones*, 1968; *Holdeman and Foss*, 1975; *Giger et al.*, 1991, *Dracos et al.*, 1992]. However, *Dracos et al.* [1992] show that this circulation develops only near the channel mouth ($2 < x/h < 10$) and in the most shallow experiment of *Dracos et al.* [1992] (respectively, $B_0/h = 4$) recirculation is absent. In all of the *Rowland et al.* [2009a] experiments (B_0/h between 4.4 and 5), the vertical velocity field did not have a sufficient resolution to determine whether the recirculation was present or not.

2.1. Stability Analysis of Shallow Jets

Linear stability analysis has being widely employed to find the stability threshold of shallow jets, wakes, and mixing layers [*Jirka*, 1994; *Socolofsky and Jirka*, 2004; *Chen and Jirka*, 1998; *Jirka*, 2001; *van Prooijen and Uijttewaal*, 2002; *Socolofsky and Jirka*, 2004]. In these studies a parallel flow is considered, and a linearization of the shallow water equations yields a modified Orr-Sommerfeld equation, which includes turbulence viscosity (ν^T) and bottom friction (c_f) as dissipative terms. Analyses of this type have shown that jet stability depends on the turbulent Reynolds number $Re_h = uh/\nu^T$ and on the stability number S:

$$S = c_f \frac{L}{h} = \frac{c_f}{2}\frac{b_0}{h}, \tag{6}$$

where h is the water depth, L is a jet length scale which for expanding jets is taken equal to the half width of the river mouth b_0 [*Jirka*, 1994], c_f is the friction factor, and u is the local one-directional velocity. Note that shallow water equations more often employ a Chezy coefficient C that can be written as $C = \sqrt{2g/c_f}$. For shallow wakes *Chen and Jirka* [1998] discovered that for $Re_h > 10^3$ viscous effects can be neglected and stability depends only on S. For very high Re_h (inviscid conditions) a critical value of $S_c = 0.69$ is found, which drops to about 0.5 for typical viscid conditions [*Chen and Jirka*, 1998; *Socolofsky and Jirka*, 2004]. Note that the hypothesis of parallel streamlines at the base of the linear analysis results in neglecting any spreading of the jet. A fully nonlinear quasi-three-dimensional analysis has been recently performed by using the numerical model Delft3D [*Canestrelli et al.*, 2014]. The results of numerical simulations indicate a strong influence of the nondimensional number S on jet stability, and a somewhat milder dependence on a mouth Reynolds number defined as

$$Re_B = \frac{U_0 B_0}{\nu}, \tag{7}$$

where ν is the molecular viscosity. *Canestrelli et al.* [2014] performed a series of numerical experiments and determined the critical stability number S_c at which the jet becomes unstable over ranges of Re_B values spanning both laboratory and natural dimensions of river mouths. The stability diagram of Figure 3 shows that for large S frictional effects suppress any meandering of the jet and a stable flow is attained. The critical value of S increases with the Reynolds number and the best transition curve, obtained by a linear discriminant analysis, reads

$$S_c = 1.3 \cdot 10^{-3} Re_B^{0.235}. \tag{8}$$

The upper and lower boundaries of the transition zone (dashed lines in Figure 2) read

$$\begin{cases} S_c^{UP} = 0.9 \cdot 10^{-3} Re_B^{0.235} & (9) \\ S_c^{DOWN} = 1.9 \cdot 10^{-3} Re_B^{0.235} & (10) \end{cases}$$

The nonlinear numerical simulations of *Canestrelli et al.* [2014] yields lower values of S_c compared to those obtained by a linear analysis. This discrepancy is due to the fact that in a turbulent jet, the width increases

with distance from the inlet because of friction and lateral entrainment of water. A finite distance from the mouth (between $8B_0$ and $9B_0$) is needed for the shallow jet to change from purely three-dimensional to quasi-two-dimensional with large horizontal counter-rotating vortices [*Rowland et al.*, 2009a]. At this distance, a jet width larger than the mouth width implies a locally higher stability number that is more likely to suppress the meandering pattern.

The stability of the jet and its effect on sediment transport have important consequences for depositional patterns at river mouths and the formation of mouth bar deposits.

2.2. The Theory of Potential Vorticity Applied to Shallow Jets

In recent years several researchers have sought to determine the hydrodynamic and sediment transport conditions that lead to localized deposition at the margins of the river effluent jet, thus forming subaqueous levees [*Rowland et al.*, 2009a; *Rowland et al.*, 2010; *Falcini and Jerolmack*, 2010; *Mariotti et al.*, 2013]. Clues to these conditions are found by examining natural and experimental plumes emanating from different existing channel morphologies. This provided the basis for a new approach where geophysical fluid dynamics theories were adapted to describe river mouth jets and their related sedimentation.

The potential vorticity (PV) approach [*Pedlosky*, 1987; *Falcini and Jerolmack*, 2010; *Falcini et al.*, 2014] describes the relationship between the internal, hydrodynamic structure of the flow and its sedimentation properties. By introducing the relative vorticity of a sediment-laden jet, i.e., $\vec{\omega} = (\chi, \psi, \zeta) = \nabla \times \vec{u}$, where $\vec{u} = (u, v, w)$ is the flow velocity, and an arbitrary scalar property of the flow (λ), the general definition of PV is [*Pedlosky*, 1987]

$$\Pi_\lambda = \frac{\vec{\omega}_a}{\rho} \cdot \nabla\lambda, \tag{11}$$

where $\vec{\omega}_a = 2\vec{\Omega} + \vec{\omega}$ is the absolute vorticity, $\vec{\Omega}$ is the planetary vorticity, and ρ is the water density.

The PV definition in (11) allows one to set an ad hoc PV by considering some scalar fluid property λ that can be defined as [*Pedlosky*, 1987]

$$\frac{d\lambda}{dt} = \Psi. \tag{12}$$

Classical choices for λ in meteorology and physical oceanography are the thickness of the water/air column, the potential temperature, or the potential density of the water/air. *Falcini and Jerolmack* [2010] proposed a novel value for the scalar $\lambda = c$, where $c = c(x, y, z, t)$ represents the suspended sediment concentration (SSC) within the river jet. This allows one to formally investigate and diagnose the role of jet vorticity on suspended sediment distribution, which is essential for predicting patterns of deposition at river mouths.

With the use of the Navier-Stokes and the continuity equations, the choice proposed by *Falcini and Jerolmack* [2010] allows one to formulate the *Ertel* [1942] PV theorem for SSC as

$$\frac{d}{dt}\left(\frac{\vec{\omega}}{\rho} \cdot \nabla c\right) = \frac{\vec{\omega}}{\rho} \cdot \nabla\Psi + \frac{\nabla c}{\rho} \cdot \left[\nabla \times \left(\frac{\vec{F}}{\rho}\right)\right], \tag{13}$$

where the internal jet vorticity due to shearing ($\vec{\omega}$) is assumed to be greater than the planetary vorticity $\vec{\Omega}$ and baroclinic effects are disregarded [*Falcini and Jerolmack*, 2010]. Equation (13) expresses the temporal and spatial variations of sediment-PV, and thus describes the dynamics of a sediment-laden river jet system affected by (i) external forces ($\vec{F}$) due to both lateral and bottom shear stresses and (ii) erosional or depositional processes ($\Psi \equiv \frac{dc}{dt}$). One can therefore envision the left-hand side of equation (14) as a measure (or a probe) of the status of the flow in terms of vorticity and SSC spatial gradients (i.e., the sediment-PV), while the right-hand side (RHS) of (13) indicates the causes leading to the evolution of such a sediment-PV state.

When energy dissipation due to friction is limited and the jet structure is able to maintain sediment in suspension, sediment-PV is conserved and will decrease when the sediment settles or when the friction reduces vorticity. A meaningful example for "sediment-PV state" is easily provided by reasonably neglecting vertical velocities and the vertical gradient of the cross-stream velocity ($w = 0$ and $\partial v/\partial y = 0$).

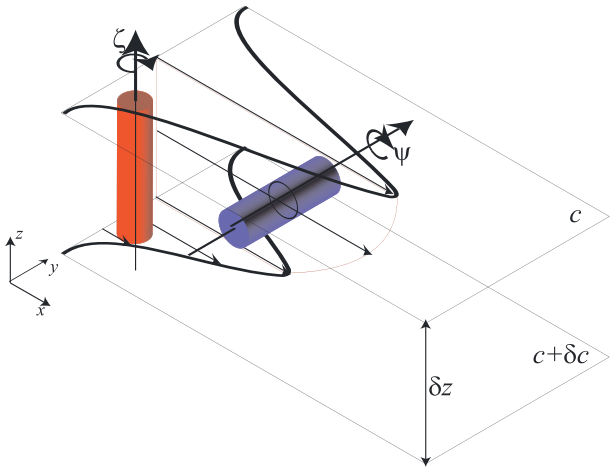

Figure 4. Schematic representation of the vorticity field $\vec{\omega} = (0, \psi, \zeta)$ in a sediment-laden, stratified jet, where the vorticity components $\psi = \partial u/\partial z$ and $\zeta = \partial v/\partial x - \partial u/\partial y$ are indicated by the blue and red cylinders, respectively. The bold lines are the horizontal velocity profile at two different depths; thin arrows indicate velocities on both horizontal and vertical planes. The horizontal planes along z represent suspended sediment stratification.

Hence, the jet vorticity is $\vec{\omega} \approx (0, \psi, \zeta)$, where $\psi \approx \partial u/\partial z$ (i.e., secondary circulations of the flow are not taken into account), and it leads to the following, simplified sediment-PV definition:

$$\rho \Pi_c = \frac{\partial u}{\partial z}\frac{\partial c}{\partial y} + \left(\frac{\partial v}{\partial x} - \frac{\partial u}{\partial y}\right)\frac{\partial c}{\partial z}. \qquad (14)$$

The first RHS term of (14) describes the coupling between vertical shear due to bottom friction that acts to maintain sediment in suspension and the lateral distribution of SSC ($\partial c/\partial y$, Figure 4). The second RHS term of (14) takes into account the horizontal velocity profile (Figure 4), i.e., lateral shearing, $\partial u/\partial y$, and spreading, $\partial v/\partial x$, of the jet (i.e., lateral momentum transport associated with lateral water entrainment) coupled with the vertical distribution of SSC ($\partial c/\partial z$). A sediment-PV state is therefore the status of the SSC distribution within the jet (vertical and lateral gradients of SSC) that results from the status of vertical and lateral shearing of the flow.

In section 4 we apply this theory to explain the relationship between gradients in suspended sediment concentration and the structure of a jet exiting a river mouth.

3. Basic Theory of Mouth Bar and Levee Formation

As seen in the previous section, the jet may be temporally stable or unstable (meandering), depending upon the jet stability parameter and inlet Reynolds number [*Canestrelli et al*., 2014]. Whether stable or unstable, it is the jet that determines sediment particle flow paths and bed deposition patterns in front of the river mouth. The evolving bed modifies the jet, giving rise to a coupled morphodynamic system.

There are two important loci of deposition in the jet region: subaqueous levees that fringe the jet and river mouth bars (RMB) that form under the jet at some variable distance from the tip of the distributary channel or river mouth. The RMBs take two end-member forms, a triangular "middle-ground" bar with two or more channels separating it from the subaqueous levees, and a crescentic, relatively unchanneled bar connecting the levee tips (Figure 1b). Little quantitative work exists on the crescentic type, and this remains an area of future research, although these deposits readily form in laboratory and numerical experiments [*Jopling,* 1963; *Bonham-Carter and Sutherland,* 1968]. Earlier workers [*Bates*, 1953; *Axelsson*, 1967] thought the origin of both bar types was self-evident: the unconfined flow of the jet causes a reduction of flow competency. Later workers [*Welder*, 1959; *Mikhailov*, 1966; *Bonham-Carter and Sutherland*, 1968; *Farmer and Waldrop*, 1977; *Wright*, 1977; *Wang*, 1985; *Izumi et al*., 1999] elaborated upon this notion by relating the bar types described above to turbulent jet theory and developing simplified process-response models. Numerous studies in the past decade have extended, refined, and in some cases, proposed alternative conceptual models for delta growth through bars and subaqueous levees [*DuMars*, 2002; *Edmonds and Slingerland*, 2007; *Edmonds and Slingerland*, 2008; *Rowland et al*., 2009b; *Edmonds and Slingerland*, 2010; *Falcini and Jerolmack*, 2010; *Geleynse et al*., 2010; *Rowland et al*., 2010; *Mariotti et al*., 2013; *Nardin et al*., 2013]. The following discussion is based upon these latter studies.

There are four stages in the formation of a river mouth bar under stable jets expanding into a shallow, sloping basin [*Edmonds and Slingerland*, 2007] (Figure 5): (1) initially, parallel subaqueous levees are deposited along the edges of the jet and a small river mouth bar grows just basinward of the channel tip; (2) the subaqueous levees continue to extend basinward and the river mouth bar progrades and aggrades; (3) river mouth bar

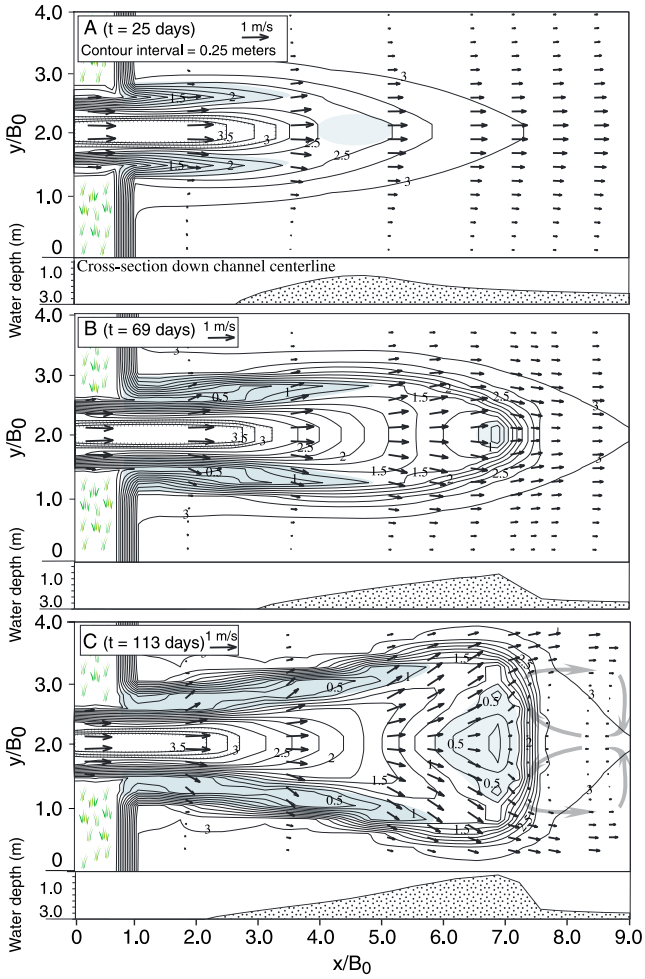

Figure 5. Serial bathymetric contour maps, longitudinal cross sections, and vertically integrated velocity vectors depicting the general evolution of a river mouth bar system under a stable turbulent jet as predicted by the morphodynamic flow-sediment transport model Delft3D [*Edmonds and Slingerland*, 2007]. (a) River mouth bar progrades to $x/W = 5$. (b) Levees continue to grow basinward but the river mouth bar stops prograding. (c) Levees begin to spread due to the presence of the river mouth bar. The river mouth bar aggrades vertically and widens.

progradation stops and the subaqueous levees continue extending and flare basinward around the stable river mouth bar; and (4) finally, the river mouth bar reaches the water surface, widens, and creates the classic subaerial river mouth bar observed in plan view.

In some cases the subaqueous levees keep extending in the receiving basin without forming a triangular mouth bar [*Canestrelli et al*., 2014; *Falcini and Jerolmack*, 2010]. This is probably due to sediment transport processes that continuously advect sediment to the side of the jet thereby promoting levee growth to the detriment of bar formation [*Mariotti et al*., 2013; *Canestrelli et al*., 2014].

River mouth bars first form within the jet where the negative gradient of longitudinal sediment flux is steepest. These gradients stem from a sharp drop in transport capacity due to jet expansion and flow deceleration. In numerical simulations with sand and both bed load and suspended sediment transport [*Edmonds and Slingerland*, 2007; *Canestrelli et al*., 2014] this occurs at a distance between zero and two channel widths from the river mouth for stable jets and at a higher distance for unstable jets. The river mouth bar then progrades because its presence causes acceleration of flow. The point of maximum fluid acceleration occurs on the upstream bar face, leading to erosion of the face and the bar top. With an increase in depth on the backside of the bar, the pressure gradient diminishes, flow decelerates, and sediment eroded from the upstream bar face deposits. The net result is bar progradation and extension of the flanking subaqueous levees. At a certain point the bar becomes an obstacle to the flow triggering a bifurcation with the formation of two channels that laterally erode the bar deposits. With time the entire river mouth bar and subaqueous levee complex aggrades, and this sediment platform is characterized by steep slopes on its downstream and transverse margins. A low-velocity wake now exists downstream of the bar.

River mouth bars stop prograding when the depth over the bar is equal to or less than 40% of the inlet depth because fluid pressure on the upstream side of the bar is large enough to divert flow around the bar [*Edmonds and Slingerland*, 2007]. This leads to deceleration of flow over the bar and enhanced aggradation as the shear stress on the bar top falls below the critical threshold required for bed load motion. While the bar top becomes stable, the downstream flanks of the bar are still morphodynamically active.

This conceptual model based on numerical results was validated by *Esposito et al*. [2013] with field data collected in a mouth bar of the Mississippi River. In accordance with *Edmonds and Slingerland* [2007] model, *Esposito et al*. [2013] measured a general decrease in velocity across the bar top and intense

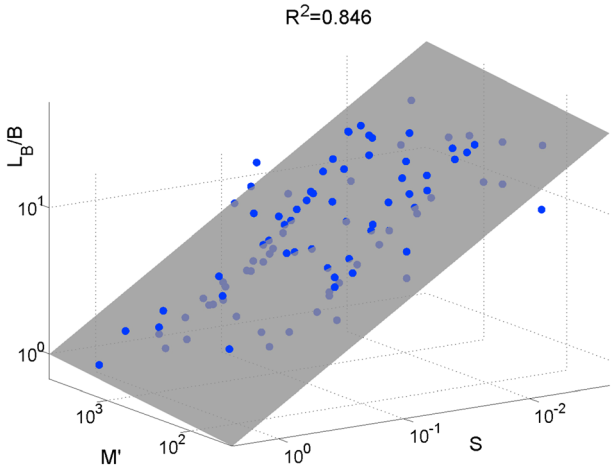

Figure 6. Dimensionless distance to river mouth bar, L_b/B, increases proportionally to the dimensionless jet momentum flux M' and inversely proportional to the stability factor S. The linear least squares planar fit is also shown.

deposition in the distal fringe of the bar accompanied to a decline in suspended material. *Esposito et al.* [2013] further extended the conceptual model of *Edmonds and Slingerland* [2007] to include shifting patterns of sediment supply and delivery triggered by variable flow discharge and tides. Three flow regimes are thus introduced: during periods of high flow, the mouth bar can be in an aggradational, progradational, or runaway aggradational phase with sand transported by the channel distributary and then deposited on the bar; when the depth of water over the bar decreases, runaway aggradation is dominant and only mud is deposited; finally, when the bar is emergent, the deposited mud consolidates reinforcing the substrate.

The equilibrium distance from the distributary channel tip to the stagnated river mouth bar was postulated by *Bates* [1953] to be about four channel widths because jet centerline velocities begin to decrease at this location due to jet spreading. This conjecture was contradicted by *Wright et al.* [1974] who collected field measurements from 10 river-dominated deltas and found that the average distance between the main river channel and the associated mouth bar is 10 channel widths, although this value decreases with increasing channel aspect ratio [*Mikhailov*, 1966]. Other workers concluded that this distance should be a function of $\frac{hU_0}{w_s}$, where w_s is the settling velocity of the sediment, or set by the point where the bed shear stress falls below the critical threshold for mobility in an expanding turbulent jet [*Bonham-Carter and Sutherland*, 1967; *Wang*, 1985]. However, neither of these criteria can predict bar distances since they neglect flow dynamics and mouth bar progradation [*Edmonds and Slingerland*, 2007]. Recent results indicate that the distance from the subaerial distributary channel tip to the final stagnated bar (L_{RMB}) is a function of dimensionless jet momentum flux and jet stability number [*Canestrelli et al.*, 2014] (see Figure 6):

$$\frac{L_{RMB}}{h} = f\left[\frac{\rho U_0{}^2}{(\sigma-\rho)gD_{50}}, c_f\frac{B_0}{h}\right], \tag{15}$$

where D_{50} is the median grain diameter. The distance to the bar stagnation point is independent of shelf slope, and the limited numerical experiments in *Edmonds and Slingerland* [2007] indicate that positive buoyancy of the jet has little noticeable effect on this distance. Compared to stable jets, in unstable jets the mouth bars stabilize much farther offshore [*Canestrelli et al.*, 2014]. This increase arises because the augmented lateral diffusion of sediment forms more robust subaqueous levees, thereby confining the turbulent jet. In this case the distance depends more upon the jet stability number than the jet momentum flux or potential vorticity, as introduced in the following section. A detailed comparison between the results presented in *Canestrelli et al.* [2014] and field measurements is still needed to fully validate this novel theory.

4. The Role of Potential Vorticity and Sediment Eddy Diffusivity on the Dynamics of River Mouth Deposits

The model of river mouth bar formation outlined above can be better understood by using sediment-PV as a diagnostic tool to look at areas within the jet with high gradients in sediment concentration and high vorticity. It is therefore clear that sediment-PV gives some indication of sediment transport or deposition across the jet, consequently exerting a control on spatial depositional patterns [*Falcini and Jerolmack*, 2010]: low-PV systems (marked by rather "flat" lateral and vertical profiles of both velocity and SSC) are associated with diffuse jets and mouth bar deposition, conditions that brings to bifurcating channels and a

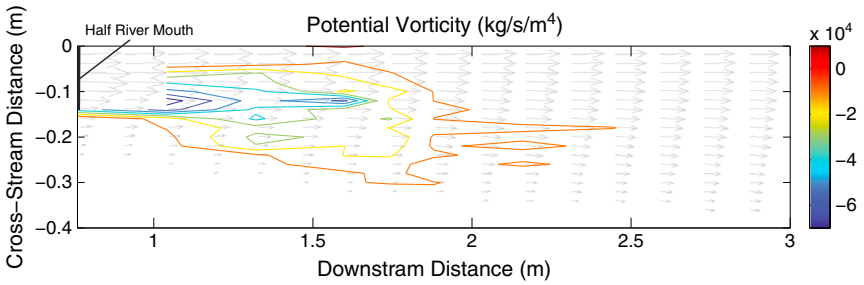

Figure 7. PV contours (kg/s/m^4) as calculated from *Rowland et al.*'s [2009a] experimental data for half of the sediment-laden jet (0 m in the cross-stream direction corresponds to the centerline of the jet). The horizontal, time- and depth-averaged velocity field (gray arrows) is superimposed (maximum velocity = 50 cm/s). Negative PV values indicate a clockwise rotation of the fluid from the centerline out toward the margin. The flow field was measured before the formation of the levee.

radial growth plan [*Edmonds and Slingerland*, 2007]; high-PV jets (marked by pronounced lateral and vertical profiles of both velocity and SSC) exhibit little spreading, a condition that suppresses deposition at the center of the jet, thus leading to elongate levees [*Falcini et al*., 2014].

The sediment-PV distribution was used by *Falcini et al*. [2014] to seek a mechanistic relationship between flow characteristics and depositional patterns. After analyzing the experiments of *Rowland et al.* [2009a], these authors inferred suspended sediment transport property of the flow by mapping the sediment-PV and concluded that (Figure 7):

1. The steady state sediment-PV cross-stream distribution shows a peak at the two outlet margins (Figure 7). These PV peaks reveal that the horizontal velocity profile, captured by ζ, locally affects the lateral SSC distribution, namely $\partial c/\partial y$, as experimentally noted by *Rowland et al*. [2009a]. Such a sediment-PV peak can be recognized in the downstream evolution of the lateral shear stress profile.
2. The steady state sediment-PV pattern is maintained for about 7–7.5 mouth widths downstream (Figure 7) before it fully decays. This distance marks the passage between a transitional low-mixing rate zone and the Zone of Established Flow (ZOEF), where turbulence generated by shearing along the margins of the jet penetrates to the jet core [*Bates*, 1953; *Rowland et al*., 2009a].

Falcini et al. [2012] monitored velocity and SSC (and thus sediment-PV) of the Mississippi River plume during the Historic 2011 Flood from remote sensing and in situ hydrographic and sediment data. The sediment-PV constancy that characterized the low-spreading jet was thus verified for the Mississippi River southwest pass, a natural system that exhibits a strong levee deposition and that delivers a large amount of suspended sediment offshore [*Kim et al*., 2009a; *Edmonds and Slingerland*, 2010; *Falcini and Jerolmack*, 2010].

A fundamental role in the depositional patterns resides in the intrinsic jet's ability to maintain its filamentous shape. Jets characterized by high PV tend to remain confined and deliver sediment to the margins since sediment-PV indicates the potential for lateral advection of sediments through the generation of vortices [*Mariotti et al*., 2013]. Sediment-PV, in sum, combines velocity shear and sediment concentration gradients for steady flows and thus clarifies, from theory, their combined role in building elongated channels at river mouths.

However, *Canestrelli et al*. [2014] argue that the hypothesis of PV conservation is valid only for a deep and narrow river mouth, where energy dissipation due to friction is limited. In such circumstances, PV is equivalent to jet momentum. When instead friction is dominant, the main process controlling the formation of lateral levees is jet stability, which is regulated by the stability parameter S. In fact, the PV approach described in the previous section approximates the turbulent jet as a steady flow, neglecting unsteady coherent structures (i.e., meanders with a horizontal scale $\sim B_0$ and time scale of $\sim B_0/U_0$) that are also related to the formation of lateral levees [*Rowland et al*., 2009a].

Recent laboratory experiments [*Rowland et al*., 2009a] showed that jet instability, characterized by large-scale meanders, increases the sediment eddy diffusivity, i.e., the tendency to transfer sediment to the side of the jet and hence to build lateral deposits [*Rowland et al*., 2010].

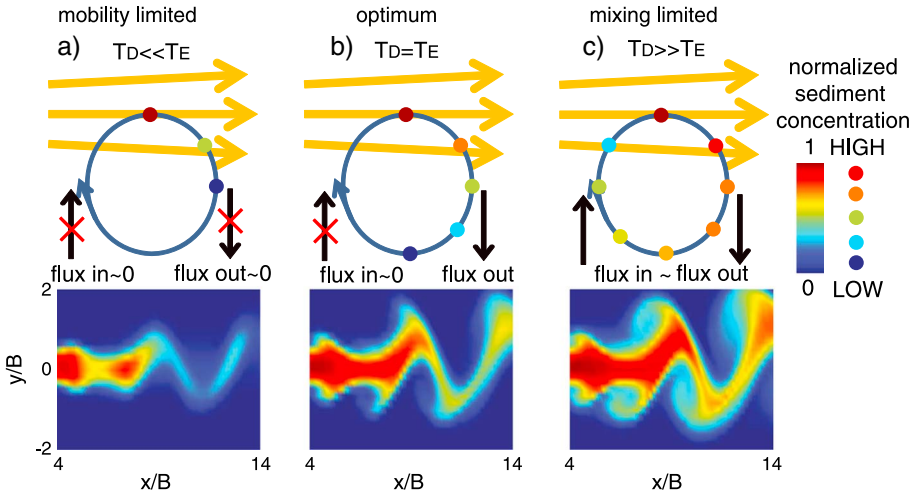

Figure 8. Conceptual model of sediments transported on an eddy. (a) For $T_D < T_E$, sediments are deposited as soon as they exit the centerline, resulting in a low-eddy diffusivity. (b) For $T_D \sim T_E$, sediments are deposited at the extreme end of the eddy, resulting in the highest sediment eddy diffusivity. (c) For $T_D > T_E$, particles are deposited after the eddy has begun the inward phase or are not deposited at all, resulting in a low sediment eddy diffusivity, as suggested by *Rowland et al.* [2010]. The figures on the bottom are snapshots of the concentration field ($d50 = 324$, 144, and 64 μm) at the same time, with $h = 1$ m, $U = 2.0$ m/s, $W = 6$ m. Color scale of the concentration is normalized by the equilibrium concentration at the outlet [from *Mariotti et al.*, 2013].

Mariotti et al. [2013] further tested this hypothesis with a series of numerical simulations with the model Delft3D. In these simulations an unstable turbulent jet is exiting an outlet carrying sand of variable grain size in suspension. Eddy viscosity, sediment eddy diffusivity, and deposition patterns were spatially analyzed at high resolution both within the jet and outside of it. Both *Rowland et al.* [2010] and *Mariotti et al.* [2013] suggested that the enhancement in sediment eddy diffusivity is caused by the peculiar dynamic of the sediments that are trapped in the large-scale eddies, which act as a "conveyor belt" (Figure 8). If the settling time scale, i.e., the time needed for the sediment to reach the bed, $T_D = h/(2w_s)$, is comparable to the meandering time scale, i.e., the time needed for a meander to complete a half revolution, $T_E = B_0/(0.07\,U_0)$, sediments settle at the farthest distance from the centerline [*Mariotti et al.*, 2013]. If the settling time scale is significantly greater than the meandering time scale, sediments move back and forth within the eddy, effectively reducing the eddy diffusivity [*Rowland et al.*, 2010; *Mariotti et al.*, 2013]. *Mariotti et al.* [2013] pointed out that if the settling time scale is much shorter than the meandering time scale, sediment cannot exploit the eddy conveyor belt, and it will tend to deposit close to the centerline.

Rowland et al. [2009a] experiments showed that when jet instability is suppressed, levee formation ceases and central deposition is favored. *Mariotti et al.* [2013] suggested that a stable jet is a limit case of an unstable jet with a deposition time scale much smaller than the eddy time scale, i.e., a condition in which sediments cannot exit the jet core by using the eddy conveyor belt. Such a prediction was confirmed by *Canestrelli et al.* [2014], who showed that the degree of jet instability, quantified by the stability parameter S, determines the jet's ability to build lateral levees. Interestingly, in this regime defined by *Mariotti et al.* [2013] as "mobility limited" (because the sediments are not transported by the large-scale eddies) the ability to build lateral levees increases with the ratio T_D/T_E, i.e., for a fixed velocity and sediment size, and consequently, it increases with the aspect ratio h/B_0, which is proportional to the inverse of the stability parameter. Moreover, levee formation occurs when a decrease of T_D is followed by a decrease of T_E, which would correspond to high vorticity since $\zeta \approx U_0/B_0 \approx 1/T_E$. Therefore, this result is also in agreement with the observations based on PV theory.

In conclusion, jet instability controls the overall morphodynamics of the river mouth and determines the prevalence of lateral levees with respect to a central bar. PV has instead a limited role on the overall shape of the deposit [*Canestrelli et al.*, 2014]. PV can be used to map within the flow field areas where large eddies form (due to high vorticity) and sediment is more prone to deposition (because of high

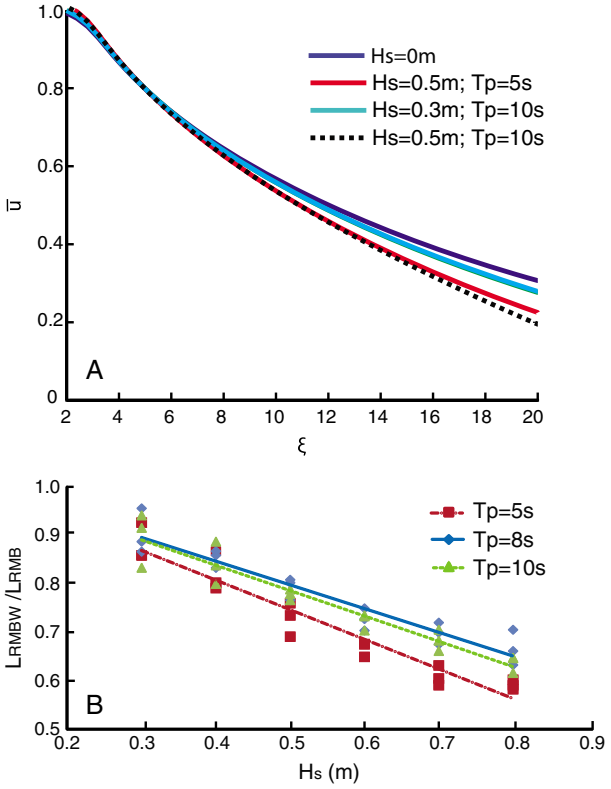

Figure 9. (a) Normalized longitudinal velocity ($\bar{u} = u/U_0$) along the jet centerline exiting a river mouth computed with the model Delft3D-SWAN for different wave conditions (H_s is the wave height and T_p the peak period). A reduction in centerline velocity indicates that the jet is spreading. (b) Normalized mouth bar stagnation distance (L_{RMBW}/L_{RMB}) as a function of significant wave height [after *Nardin et al.*, 2013].

gradients in sediment concentration). PV can therefore determine the position of the forming lateral levees (Figure 7). The application of potential vorticity to sediment transport and related depositional patterns is still at its infancy; future research will likely increase the applications of this powerful tool.

5. Wave Influence on River Mouth Deposits

Traditionally, higher wave activity tends to be associated with single-channel deltas that do not bifurcate. This has led to the suggestion that energetic waves propagating from offshore suppress mouth bar formation [*Jerolmack and Swenson*, 2007]; in the same way they diffuse and smooth shoreline perturbations. On the other hand, recent results show that short waves ($H_S < 1$ m, $T < 10$ s) promote mouth bar growth in shallow bays [*Nardin et al.*, 2013]. This occurs because waves decrease the time of bar formation, reduce its distance from the river mouth, and increase the bar width-to-length ratio. Wave influence on mouth bar growth is therefore complex: small waves promote mouth bar formation via increased jet spreading; large waves suppress mouth bar formation.

To determine the effect of small waves ($H_s < 1$ m) on river mouth deposits, *Nardin et al.* [2013] considered a homopycnal river plume subject to frontal wave attack. They developed an analytical model for the hydrodynamic interaction between incoming waves and a turbulent expanding jet based on the theory of *Ozsoy and Unluata* [1982] and compared the results with the numerical model Delft3D coupled to the wave module SWAN (Simulating WAves Nearshore) [*Booij et al.*, 1999]. Both the analytical model and Delft3D predict that incoming surface gravity waves increase the spreading of the jet (Figure 9a) and that the interaction between wave and current boundary layers causes an increase in bottom friction. Numerical results indicate that, in the presence of waves, mouth bars form up to 35% closer to the mouth (Figure 9b).

Waves affect the longitudinal velocity, decreasing the velocity in proximity of the centerline while increasing it in regions far from the jet core (Figure 9a). To quantify the role of bottom shear stress on jet spreading, *Nardin et al.* [2013] included the contribution of wave bed shear stress in the theory of *Ozsoy and Unluata* [1982] by adding a parameter m that represents the ratio between the combined bed wave/current shear stress and the shear stress due to the current only. The approximate momentum equation becomes

$$\frac{\partial hu^2}{\partial x} + \frac{\partial huv}{\partial y} = -\frac{gu^2}{C^2}m + \frac{1}{\rho}\frac{\partial \tau_{yx}}{\partial y} \tag{16}$$

with

$$m = \frac{\tau_m}{\tau_c} = 1 + 1.2\left(\frac{\tau_w}{\tau_w + \tau_c}\right)^{\frac{3}{2}}, \tag{17}$$

where τ_m is the combined waves/current bed shear stress, and current, τ_c, and wave, τ_w, bed shear stresses are computed as follows:

$$\tau_c = \frac{g\rho u|u|}{C^2}\,, \tag{18a}$$

$$\tau_w = \frac{1}{2}\rho f_w u_b^2\,, \text{ and} \tag{18b}$$

$$u_b = \frac{\pi H_s}{T_p \sinh(Kh)}, \tag{18c}$$

where u_b is the significant wave bottom orbital velocity, K is the wave number, H_s is the significant wave height, T_p is the wave peak period, and f_w is a wave friction coefficient. Assuming that the wave-induced bed shear stress is uniform within the domain, the ratio m is high where the current shear stress is low, i.e., far from the river mouth, and low where the current shear stress is high, i.e., close to the jet core. A higher m results in more friction and in an increase in jet spreading, which occurs far from the mouth, where the effect of waves is stronger (equation (16)).

Waves have therefore two important effects on the turbulent jet that might influence the morphodynamic evolution of a mouth bar. First, the presence of waves enhances jet spreading, which reduces the centerline velocity and shear stress (Figure 9a). Second, the presence of waves increases the total maximum shear stress, τ_{max}, by adding the shear stress produced by wave orbital velocities at the bottom, τ_w, to the current shear stresses, τ_m.

Nardin et al. [2013] showed through numerical experiments that the increase in shear stress triggered by waves is greater than the reduction in current shear stress caused by a wave-induced increase of jet spreading.

More importantly, the distance to the mouth bar is always shorter in the presence of waves than in the case without waves, demonstrating that, for the parameters considered in their study, the spreading effect is always dominant with respect to the increase in bottom shear stresses. This is because deposition of sediments is governed by gradients in velocity, so that if the velocity decreases, part of the sediment in suspension settles at the bed. Bottom shear stresses are instead the driving process for resuspension and erosion, which are less important in a depositional setting like a river mouth.

In a separate study *Nardin and Fagherazzi* [2012] showed that waves and the direction from which they approach a river mouth play an important role in the distribution of sediments and related deposits. In a series of numerical experiments carried out with the model Delft3D coupled with SWAN waves affect bar development in two ways: by modifying the direction of the river jet and by changing the bottom shear stress at the river mouth and hence increasing jet spreading. *Nardin and Fagherazzi* [2012] further determined that high-angle waves with long periods prevent the formation of mouth bars; in particular, wave angles with respect to the coast between 30° and 45° are the least favorable to bar formation, producing instead a deflected river mouth.

In sheltered bays and estuaries where only locally generated waves are present, mouth bars are larger (viz., the first moment of the distribution of sediment thickness in the lateral direction is higher) when formed during wave attack because higher bottom shear stresses redistribute the sediments over a wide area. Moreover, when the depth over the bar is small enough to generate wave breaking, the sediment is laterally distributed by currents triggered by radiation stresses. Mouth bars also form faster (i.e., the time it takes for the bar to emerge is lower) when waves are present due to the enhanced spreading angle.

This is in contrast to what occurs in sediment deposits in front of tidal inlets (ebb deltas), which are reduced when large waves propagating from offshore are present, partly due to their erosive effect and partly due to long-shore currents [*Hayes*, 1980; *de Swart and Zimmerman*, 2009]. Waves have therefore a double effect on river mouth deposit; when they are small and locally generated, they favor mouth bar development, while large, swell waves inhibit their formation.

Four possible distinct morphologies stem from the combination of wave angle and the relative strength of waves with respect to the river flow [*Nardin and Fagherazzi*, 2012, Figure 10]. To quantify the relative

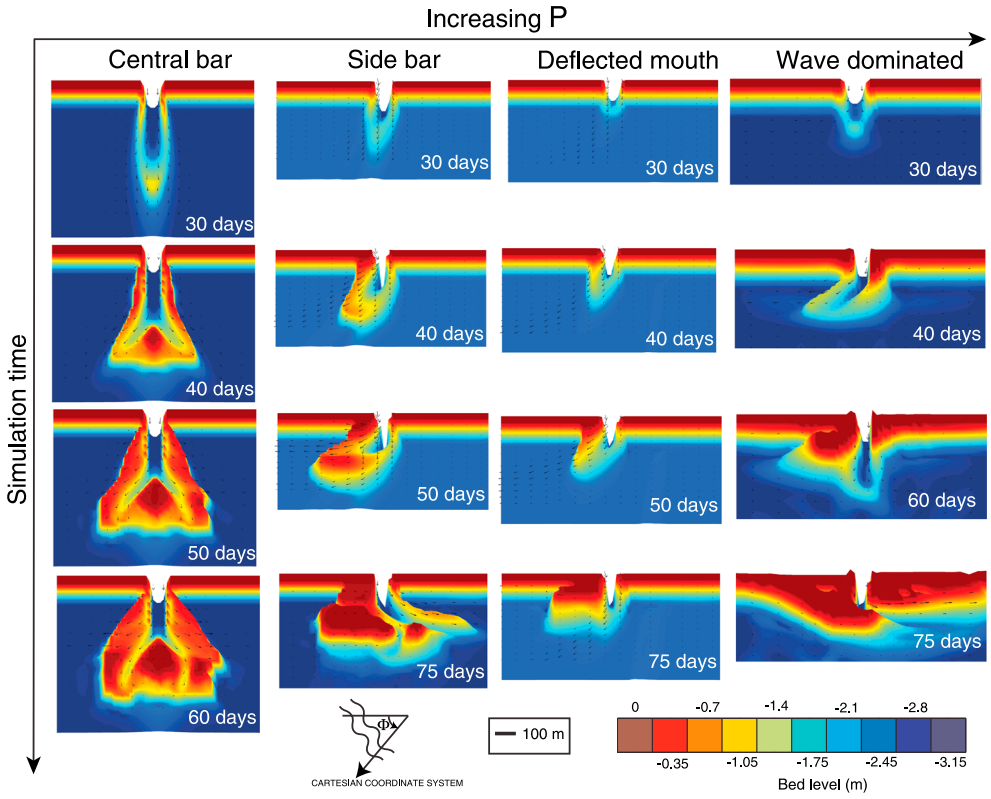

Figure 10. Snapshots from four model runs showing the evolution of a river mouth under different wave climates. Each series consists of four images of a subaqueous mouth bar evolving for 16.5 years. P is the ratio of the wave shear stress and the current shear stress at the river mouth. The velocity vectors are superimposed on the bathymetry. (first column) Central bar case with $h = 3$ m, $U_0 = 2.0$ m/s, $\Phi = 0°$, $H_S = 0.3$ m, and $T_P = 5$ s. (second column) Side bar case with $h = 3$ m, $U_0 = 1.4$ m/s, $\Phi = 30°$, $H_S = 0.5$ m, and $T_P = 10$ s. (third column) Deflected mouth case with $h = 3$ m, $U_0 = 0.8$ m/s, $\Phi = 45°$, $H_S = 0.5$ m, and $T_P = 8$ s. (fourth column) Wave-dominated case with $h = 3$ m, $U_0 = 1.0$ m/s, $\Phi = 0°$, $H_S = 1.0$ m, and $T_P = 10$ s.

importance of waves, *Nardin and Fagherazzi* [2012] introduced a nondimensional number P equal to the ratio of the wave shear stress of the incoming waves and the current shear stress at the river mouth:

$$P = \frac{\tau_w}{\tau_c}. \tag{19}$$

For weak wave conditions ($P < 0.06$), irrespectively of wave angle, the bar forms at the center, producing a bifurcation of the flow similar to the case without waves. When moderate waves ($0.06 < P < 0.6$) propagate ashore at an angle, the bar forms on the other side of the river mouth, where waves are not propagating ashore (side bar case, Figure 10). The bar still triggers a bifurcation of the flow and the formation of two channels. In time the channel closer to the shoreline silts up and the flow is concentrated in only one channel. Strong waves ($P > 0.6$) with a small angle deflect the river mouth, leading to a jet that flows parallel to the shoreline. In this case large quantities of sediments are deposited between the jet and the shoreline, producing a swash bar that extends along the coast. A fourth case occurs when strong waves reach the mouth perpendicular to the shoreline, destabilizing the jet. The jet starts oscillating, spreading sediments on a vast area without forming a distinct bar.

Recently other researchers have explored how waves affect the growth of the entire delta. While they did not include mouth bar growth in their model, *Ashton and Giosan* [2011] showed that waves approaching from one direction can lead to the asymmetric evolution of a delta, with the possible formation of offshore extending spits and alongshore sand waves. At the time scale of the entire delta formation, wave propagating from offshore has an effect on sediment transport that is not directly associated with jet hydrodynamics. For instance, waves acting during low river discharge promote sediment reworking and reduce shoreline rugosity [*Bhattacharya and Giosan*, 2003].

Waves can also transform mouth bars into shore parallel barrier islands [*Bhattacharya and Giosan*, 2003]. Many barrier islands and spits may be better reinterpreted as components of large-scale asymmetric wave-influenced deltaic systems. *Bhattacharya and Giosan* [2003] proposed a model based on a reevaluation of several modern deltas examples (e.g., Danube, Nile, Brazos, and Guadiana) by an asymmetry index A, defined as the ratio between the net long-shore transport rate at the mouth and river discharge. Asymmetry is favored in deltas with an index $A > 200$. Bayhead deltas, lagoons, and barrier islands form naturally in prograding asymmetric deltas ($A > 200$) and are not necessarily associated with transgressive systems.

6. Tidal Influence on River Mouth Deposits

The effect of tides on river mouths is a complex phenomenon due to the interaction between riverine and tidal flow [e.g., *Cai et al*., 2013; *Lanzoni and Seminara*, 1998]. Tides affect the hydrodynamics of the jet exiting the river mouth and therefore have important consequences from a morphodynamic point of view. Depending on the relative strength of river inertia with respect to tidal energy, different hydrodynamic processes dominate the sediment deposits with consequent development of distinct morphologies.

Tidally dominated systems are characterized by a predominance of coast-normal, elongate tidal bars, while wave-generated, coast-parallel barriers and/or beaches are rare. When the tidal discharge is much higher with respect to the fluvial one, elongated deposits form due to tidally induced bidirectional sediment transport, parallel to the river outflow. These elongated ridges replace more continuous mouth bars deposits and are, for example, present at the mouths of the Ganges-Brahmaputra, Shatt-al-Arab, and Fly Rivers [e.g., *Wright*, 1977; *Dalrymple and Choi*, 2007]. Differently than fluvial bars, in the absence of any riverine flow, elongated tidal bars have been found to be nonmigrating features in the mean [*Seminara and Tubino*, 2001; *de Swart and Zimmerman*, 2009]. To date, conceptual and numerical models are unable to reproduce the cyclic, elongated bars present at the mouth of macrotidal deltas [e.g., *Dalrymple et al*., 2003].

Leonardi et al. [2013] analyzed the effect of microtidal and mesotidal conditions at rivers mouths for two end-member configurations, i.e., a fluvial-dominated case in which the river discharge is constant and the tidal discharge is zero and a tidal-dominated case in which the river discharge is small compared to the oscillating tidal discharge and flow reversal is present in the river channel.

The fluvial-dominated case is typical of systems having a negligible tidal prism or during floods when the river flow is high enough to prevent flow reversal. Under these conditions the presence of tides increases jet spreading and results in a progressive wave near the river mouth, with maximum velocity occurring at low tide [*Leonardi et al*., 2013]. For this configuration the system essentially behaves like a turbulent jet debouching into a basin of varying water depths set by the tide. The jet width continuously varies throughout the tidal cycle, since it depends on bottom friction which in turns is modified by water depth [e.g., *Abramovich*, 1963]. Moreover, the relationship between water depth and jet width is not linear [*Leonardi et al*., 2013] and an increase in jet width at low tide is larger and not compensated by the corresponding decrease in jet width at high tide. For this reason, on average, the presence of tides has been found to increase the spreading rate of the jet. The interaction between the riverine and tidal discharge also promotes a drawdown of the water surface profile at low tide [e.g., *Lamb et al*., 2012]. This drawdown profile triggers an acceleration of the flow that favors the development of outward tidal residual currents and the shift from a stationary wave to a progressive wave.

From a morphological point of view, mouth bars in the presence of tides and in the fluvial-dominated case are similar to the bars forming without tides, although they are wider and shallower and show a faster initial growth rate. This is because at low tide even an incipient mouth bar becomes an obstacle to the flow, and as a consequence, strong currents establish at the two sides of the bar and promote lateral spreading of sediments.

In the tidal-dominated case the presence of a riverine discharge, albeit small if compared to the tidal discharge, leads to a temporal asymmetry of the velocity at the river mouth. As a consequence, throughout the tidal cycle, there are time intervals in which the system behaves as in the fluvially dominated case. From a morphological point of view, the final mouth bar displays features that are intermediate between tidal inlets and river-dominated mouth bars (Figure 11). An ebb-dominated

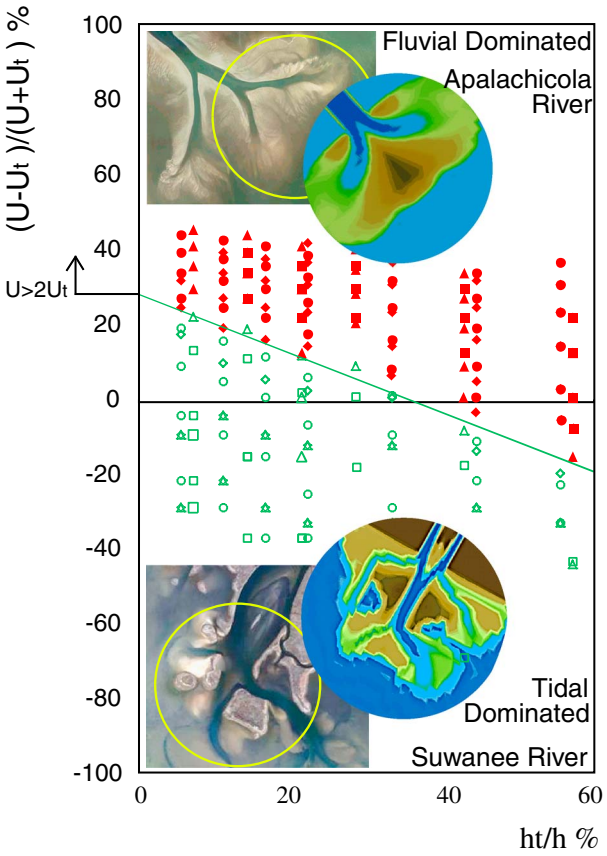

Figure 11. Morphology of river mouth deposits as a function of the nondimensional tidal amplitude (h_t/h) and the relative ratio between fluvial and tidal velocity $(U - U_t)/(U + U_t)$. Green symbols represent numerical simulations characterized by the formation of a central channel while red symbols are simple bifurcations. Circles $C = 45\ m^{1/2}/s$, $h = 4.5$ m; diamonds $C = 30\ m^{1/2}/s$, $h = 4.5$ m; triangles $C = 45\ m^{1/2}/s$, $h = 3.5$ m; squares $C = 30\ m^{1/2}/s$, $h = 3.5$ m. The insets present a qualitative comparison between numerical model results and two real systems: Apalachicola River, Florida, USA (fluvial-dominated system), and Suwanee River, Florida, USA (tidal-dominated system) [*Leonardi et al.*, 2013].

central channel, typical of tidal inlets [e.g., *Fitzgerald*, 1996; *Fitzgerald et al.*, 2006; *D'Alpaos et al.*, 2010], forms together with two lateral channels [*Leonardi et al.*, 2013]. These three channels are produced by different patterns of ebb and flood currents, with radial inflow during flood and a jet-like flow during ebb. In tidal inlets the central channel is therefore ebb dominated while the lateral channels are flood dominated [*de Swart and Zimmerman*, 2009]. A review of recent modeling results of tidal inlets indicate that ebb deposits can be asymmetric, due to either littoral drift or to the presence of alongshore tidal currents in phase with the inlet discharge [*de Swart and Zimmerman*, 2009]. On the contrary, in a tidally dominated river mouth the lateral channels are ebb dominated due to the effect of the riverine discharge [*Leonardi et al.*, 2013].

The transition from fluvially to tidally dominated conditions is dictated by the relative strength of the riverine flow with respect to the tidal flow and by the ratio between water depth and tidal amplitude (Figure 11). Fluctuations in discharge caused by the tide favor the formation of a central channel; on the other hand, oscillations in the water level in the basin promote the formation of two lateral channels. Thus, a large tidal prism and small tidal amplitudes are favorable to the establishment of a morphology typical of tidal inlets. These conditions are common in rivers dissecting flat coastal plains, where the tide can propagate upstream for a long tract thus increasing the tidal prism.

On the other hand, high tidal amplitudes and a small tidal prism maximize the drawdown effect at the river mouth, promoting fast flows at low tide and the formation of a central bar. For a river discharge larger than twice the tidal discharge, a simple bifurcation occurs independently of the tidal amplitude (Figure 11).

7. The Effect of Buoyancy

The role and relative influence of buoyancy on the evolution of river mouth deposits remains largely unexplored by physical and numerical modeling studies. This lack of emphasis on the role of outflow buoyancy stands in stark contrast to the prominent role buoyancy was hypothesized to play in the long-standing conceptual models of *Wright and Coleman* [1974] and *Wright* [1977].

The observational basis for the buoyant effluent-derived river mouth morphology of *Wright* [1977] was founded on observations of mouths of river channels of the Mississippi River delta, USA [*Wright and Coleman*, 1974]. Based on observations at the South Pass of the Mississippi River Delta, *Wright and Coleman* [1974] argued that lateral flow convergence, from the margins to the center, beneath a

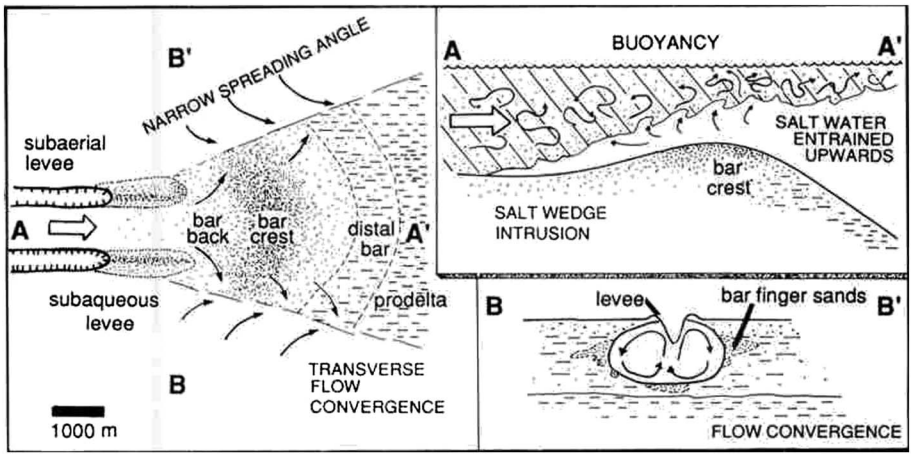

Figure 12. River mouth morphology and flow dynamics associated with buoyant river discharges as presented in *Wright* [1977] (figure from *Orton and Reading* [1993]).

debouching buoyant effluent restricts lateral divergence of sediment transport and results in the development of nearly parallel subaqueous levees. This convergent flow was attributed to the combined influence of saltwater entrainment into the flow and the development of paired helical flow cells within the buoyant effluent in response to superelevation-driven spreading from the center of the flow outward (at the surface) and from the margins inward (at the base) (Figure 12) [*Wright and Coleman*, 1974].

The rate of entrainment into the discharging effluent (U_e) depends on the stability at the interface between the plume and the underlying salt wedge. This stability is in turn a function of the flow velocity of the plume (U), the thickness of the plume (h'), and the relative density of the outflow ($\gamma = 1 - \rho_f/\rho_s$), such that [*Wright and Coleman*, 1971]:

$$U_e = 3.5\times10^{-4}\left(U - 1.15(gh'\gamma)^{1/2}\right). \tag{20}$$

The outward expansion of the buoyant river discharge results in a thinning of the flow and an upward displacement of interface between sediment-laden fresh water and the underlying salt wedge. Based on the work of *Bondar* [1970], *Wright and Coleman* [1971] presented a formulation for outflow thickness (h') at any distance (x) from the river mouth based on a dynamic expansion coefficient (a) and buoyant expansion coefficient (K):

$$h'(x) = \frac{h}{(1+ax)^{2/3}}, \tag{21}$$

where $a = \frac{3}{2}\frac{Kh(h)^{1/2}}{Q}$, $K = 4/3(2g\gamma)^{1/2}\left(1-\frac{\gamma}{2}\right)$, and Q and h are the flow discharge and depth and the river mouth, respectively.

Despite the long-standing acceptance of the morphological association between narrow, single-thread, leveed channels and buoyant outflow conditions [e.g., *Bridge*, 2003], the morphodynamic validity of this conceptual model remains largely untested. While presenting a close association between buoyancy-driven flow processes in the presentation of the conceptual models [*Wright*, 1977], *Wright and Coleman* [1971, 1974] observed that the relative importance of buoyancy on outflow dynamics was highly dependent on river discharge, tides, and waves. In fact, they noted that at high discharges the flow remained attached to the bed, as far as the mouth bar, and that buoyant forces where secondary to both friction and inertia [*Wright and Coleman*, 1974]. Based on field observations [*Rowland et al.*, 2009b], physical experiments [*Rowland et al.*, 2010], and numerical simulations [*Canestrelli et al.*, 2014; *Edmonds and Slingerland*, 2010; *Mariotti et al.*, 2013], it is clear that narrow, elongate single-thread channels may readily develop in the absence of hypopycnal outflows.

In an experimental test, *Rowland et al.* [2010] compared the depositional morphologies of a homopycnal outflow to a buoyant flow ($\gamma = 0.016$) under otherwise identical experimental conditions (Figure 13). The

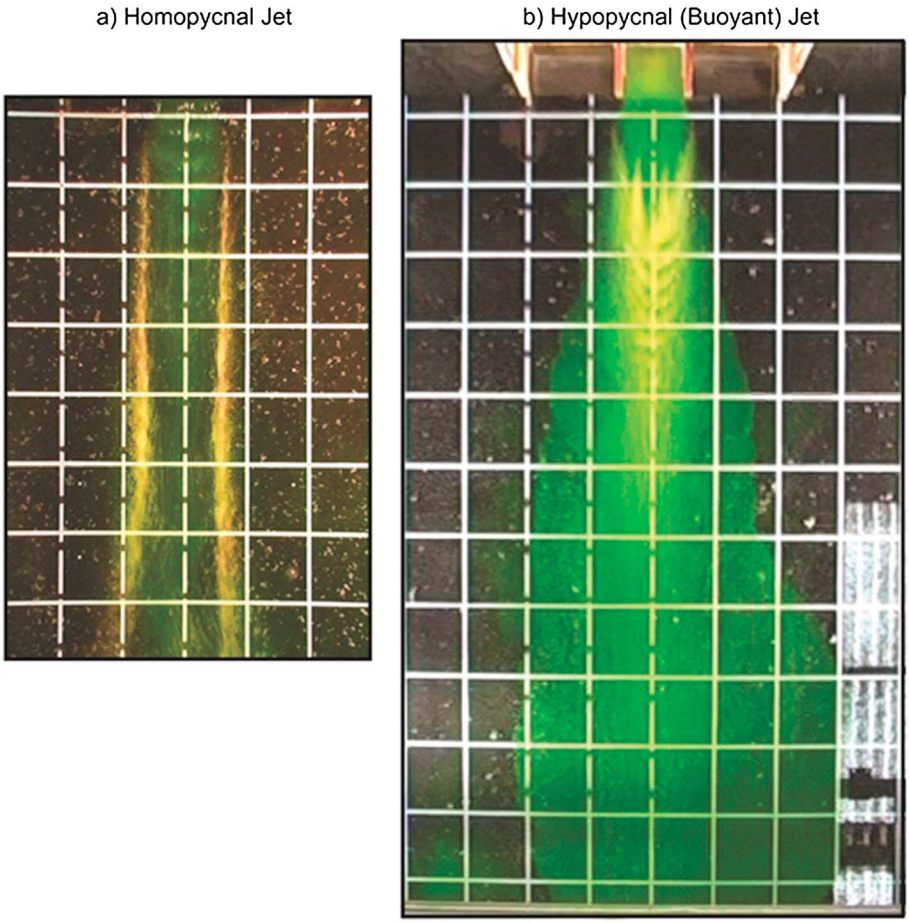

Figure 13. Overhead views of flow (highlighted in yellow) and sedimentation patterns associated with channelized discharge of (a) equal and (b) less density as the receiving basin waters. Flow was from the top to the bottom of the images, and each grid square is 20 cm by 20 cm [after *Rowland et al.*, 2010].

homopycnal outflow produced laterally bounding subaqueous levees. In contrast, rapid settling of sediment from the buoyant flow and deposition to the bed led to the rapid development of bar deposits along the axis of the flow, and separation from the bed prevented reentrainment. No development of lateral levees was observed. The flow was too thin to document the presence or absence of secondary circulation cells, but the spreading and flow patterns were qualitatively consistent with those reported for natural buoyant jets [*Fischer*, 1973]. In this experiment only a single suspended sediment grain size was used so it was not possible to determine the depositional patterns that would arise from a mixture that included finer particles with lower settling velocities.

Generalized [*Syvitski et al.*, 1988, 1998] and site-specific [*Gelfenbaum et al.*, 2009] models with buoyant river outflows into ocean settings have shown that fine-grained material ($D_{50} < 63\ \mu m$) becomes widely distributed by waves and tides, while coarser sediments are dispersed closer to river mouths. These efforts, however, have been largely aimed at broad-scale sediment dispersal and deposition patterns along coastlines or continental shelves. To date, no systematic fine-scale morphodynamic modeling study of the influence of buoyancy on outflow dynamics of river mouths has been conducted.

8. The Effect of Sediment Cohesion and Vegetation

In the most general sense, both sediment cohesion and vegetation influence river mouth deposits by stabilizing the sediment surface. Cohesion stabilizes the sediment due to intermolecular forces among particles that make them harder to erode once they are deposited and aged [e.g., *Black et al.*, 2002]. In the case of vegetation, stabilization arises from belowground roots that can withstand higher tensile

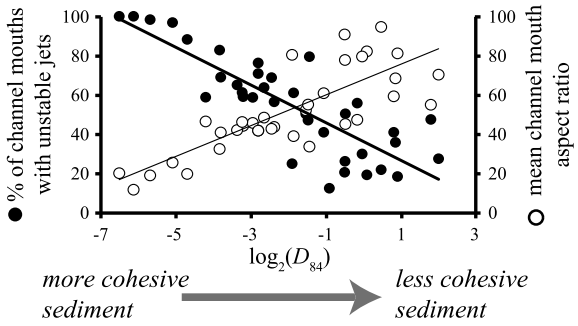

Figure 14. Modelling results from *Caldwell and Edmonds* [2014] show that as incoming sediment load becomes coarser (less cohesive sediment), the river mouth aspect ratio increases and the percent of channels with unstable jets decreases. Data are plotted against the D_{84} (84th percentile) of the incoming grain size distribution, which is proxy for percent cohesive sediment because distributions with large D_{84} have smaller proportion of grains below the cohesive threshold of 64 μm (see *Caldwell and Edmonds* [2014] for more detail). Data points correspond to average channel mouth conditions for a given self-formed delta simulation.

stresses and increase material strength [*van Eerdt*, 1985; *Hey and Thorne*, 1986; *Huang and Nanson*, 1997] and from dense aboveground biomass that diminishes turbulent kinetic energy in the flow [e.g., *Nepf*, 1999], thereby increasing deposition and reducing sediment erosion [*Fagherazzi et al.*, 2012]. Enhanced accretion triggered by vegetation can lead to the emergence of mouth bars that thus becomes deltaic islands. This process can be accelerated by production of belowground organic material (roots and rhizomes) [*Mudd et al.*, 2010].

The enhanced stabilization from sediment cohesion and vegetation also changes the hydraulic geometry of the river mouth thereby altering the hydrodynamics of the turbulent jet (equations (6) and (7)). For example, all else being equal, stabilization of river mouth levees from either sediment cohesion or vegetation reduces bank erosion and creates narrower and deeper channels [*Camporeale et al.*, 2013, and references therein]. The width-to-depth ratio of a river is a key parameter for river morphodynamics [e.g., *Zolezzi et al.*, 2012].

Recent numerical and physical modeling [*Hoyal and Sheets*, 2009; *Edmonds and Slingerland*, 2010; *Caldwell and Edmonds*, 2014] has confirmed that sediment cohesion influences river mouth dynamics because it affects the aspect ratio of the river mouth (i.e., the ratio of width to depth) leading to different turbulent jet characteristics and different depositional morphologies. *Caldwell and Edmonds* [2014] quantitatively demonstrated that the river mouth aspect ratio increases with decreasing sediment cohesion (Figure 14) using results from self-formed river deltas created in Delft3D. They also showed that decreasing aspect ratio increases the proportion of channels mouths with unstable jets (Figure 14; using criterion of *Canestrelli et al.* [2014]), leading to more river mouths that extend basinward due to fast levee growth from high lateral sediment eddy diffusivity [*Mariotti et al.*, 2013]. Along these lines, *Caldwell and Edmonds* [2014] also found that as the percent of cohesive sediment in the incoming load decreases, that is as the load becomes sandier, river mouths preferentially start creating mouth bars.

Geleynse et al. [2011] conducted similar modeling experiments of self-formed deltas using Delft3D. They also found that cohesive sediment created elongate river mouths but generated this effect with so-called "stratigraphic preconditioning" by allowing a delta to prograde over a muddy cohesive substrate rather than increasing the amount of cohesive sediment in the river. The *Geleynse et al.* [2011] results are interesting and perhaps suggest that the receiving basin stratigraphy may be important for river mouth dynamics. This result, however, is seemingly inconsistent with recent field studies on Gulf Coast deltas [*Edmonds et al.*, 2011; *Shaw et al.*, 2013] that show deltas commonly incise into the muddy cohesive substrate and yet, in the case of Wax Lake Delta, do not have elongate river mouths.

All these results suggest that cohesion may strongly influence river mouth dynamics, although there are some notable gaps in knowledge. For example, it is not clear how much cohesive sediment is necessary for river mouths to transition from creating levees to mouth bars as observed in physical [*Hoyal and Sheets*, 2009], numerical [*Edmonds and Slingerland*, 2010; *Caldwell and Edmonds*, 2014], and empirical data [*Orton and Reading*, 1993].

There is a dearth of field data on the effects of vegetation on river mouths [*Johnson et al.*, 1985; *Rosen and Xu*, 2013]. In an early study, *Johnson et al.* [1985] measured the vegetation succession on the nascent Atchafalaya delta lobe in Louisiana, USA, and found that vegetation enhanced sedimentation on levees. Using satellite data, *Rosen and Xu* [2013] found strong support for the idea that vegetation stabilizes deltaic land. In the

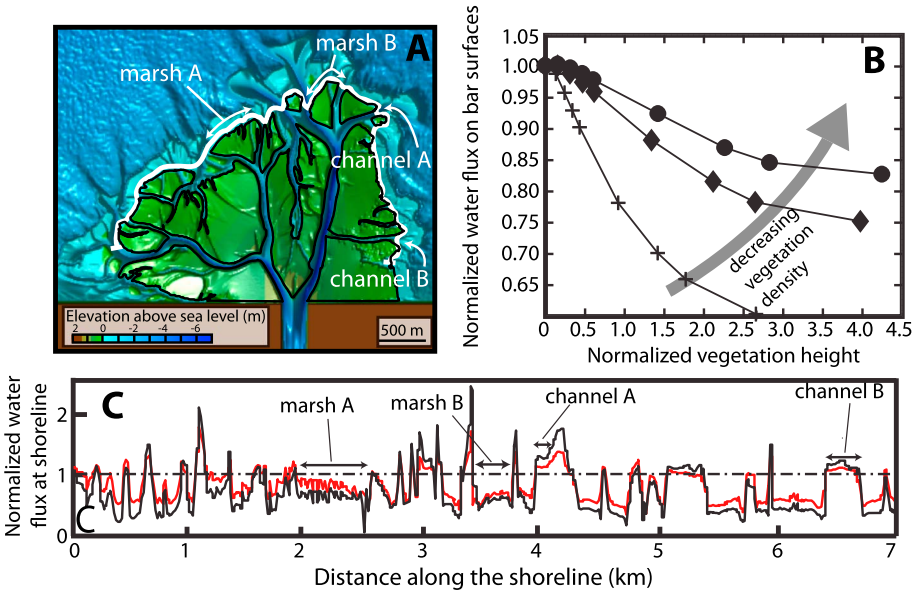

Figure 15. (a) Planform of the numerically generated delta used by *Nardin and Edmonds* [2014]. Black lines enclose bar surfaces where vegetation was placed and water fluxes were calculated. (b) When vegetation is present on exposed bars, water flux (normalized to nonvegetated conditions) over the bars decreases with increasing normalized vegetation height and increasing vegetation density. (c) The presence of vegetation forces more water into the channels and increases water flux at the channel mouths. Normalized water fluxes are calculated along the shoreline shown as white lines. Red and black lines correspond to normalized vegetation heights of 0.25 and 1, respectively. Vegetation height is normalized relative to average water depth on deltaic islands. Figure modified from *Nardin and Edmonds* [2014].

Atchafalaya and Wax Lake delta systems they measured that newly vegetated land had a ~7% chance of being converted back to open water compared to a ~32% chance for barren land.

Nardin and Edmonds [2014] performed some of the first numerical experiments exploring the effects of vegetation on deltaic river mouth dynamics during flood. Their experiments were performed on a numerically simulated delta (Figure 15a) and represented the effects of vegetation with the formulation of *Baptist* [2005], which parameterizes vegetation through the roughness coefficient; such that vegetation adds bed roughness and extracts momentum from the flow leading to a reduction in bed shear stress. They conducted 75 experiments on the same delta configuration but under different vegetation heights, densities, and flood discharges. They found that the presence of vegetation reduced the amount of water flowing over the bar surfaces by up to 25% during flood (Figure 15b). An obvious corollary of this is that the presence of vegetation on bar surfaces increases water flux through the channels. This occurs because the water seeks the smoother paths in the channels rather than the rougher, vegetated surfaces; a similar effect has also been observed in tidal marshes channels [*Temmerman et al.*, 2007]. *Nardin and Edmonds* [2014] measured the water fluxes exiting the delta at the shoreline and found that in the presence of vegetation, the water flux exiting from the channels increases, whereas it decreases elsewhere (Figure 15c). This implies that channel mouths of vegetated deltas may build land quicker and/or prograde faster since they have higher water (and presumably sediment) fluxes than their nonvegetated counterparts.

There is still much work to do on understanding the ecogeomorphic effects in deltaic environments. By comparison, numerical models of salt marsh systems suggest that the presence of vegetation greatly enhances marsh resiliency and makes them able to adapt to changes in relative sea level [*Fagherazzi et al.*, 2012]. It is not clear if the same is true for deltaic environments. Based on previous vegetation modeling studies [e.g., *Temmerman et al.*, 2007], it seems reasonable that vegetation on deltaic surfaces will increase friction, thus concentrating the flux through the channel mouths, which will potentially build land faster at the delta front. But this also means that there is less sediment per flood available for nourishing deltaic surfaces, which therefore aggrade more slowly and are more susceptible to drowning by relative sea level rise [*Nardin and Edmonds*, 2014].

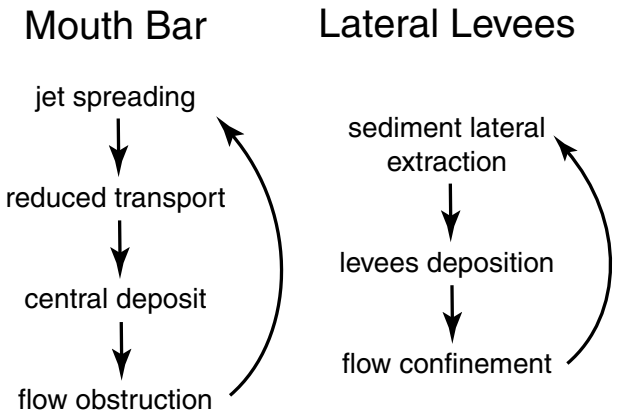

Figure 16. Hydrodynamic and morphodynamic feedbacks leading to (a) mouth bar deposition and (b) lateral levees deposition.

9. Mouth Bars or Lateral Levees?

As shown in section 3, mouth bars formation is associated with flow bifurcation. In some instances, river outflows build lateral deposits, i.e., levees, which tend to produce few single-threaded, elongated channels. Clearly mouth bar growth allows the formation of a larger subaqueous delta surface. In addition, deltas with mouth bars likely deliver sediment closer to the shoreline than a single-thread channel. Such sediments might become trapped into along-shore currents and feed distant coastal wetlands that are not directly influenced by the river hydrodynamics [*Falcini et al*., 2012]. Hence, predicting the formation of mouth bars versus lateral levees is key to understand how deltas build new and maintain existing land. We need to point out that subaqueous levees are ubiquitous even if mouth bars form (see Figure 1), so the two landforms are not mutually exclusive. Therefore, here we discuss under what conditions levees are short with a mouth bar developing in front of them or extend far in the receiving basin with or without an eventual mouth bar deposit.

Jet spreading, caused by lateral entrainment of still water and bed friction (see section 2), reduces the sediment transport capacity and enhances deposition along the centerline. Such deposition modifies the flow field, further promoting jet spreading, hence establishing a morphological feedback (Figure 16) that eventually leads to mouth bar deposition and channel bifurcation [*Bates*, 1953].

Sediment can also be extracted by the jet core and deposited at the jet lateral margins, where the bed shear stresses are lower than the critical value for transport [*Rowland et al*., 2010; *Mariotti et al*., 2013]. Such deposition tends to build lateral levees, which promote jet confinement, resulting in a morphological feedback that generates elongated channels [*Rowland et al*., 2010; *Mariotti et al*., 2013].

When a jet enters a flat basin, the initial depositional patterns do not depend on the morphological feedbacks, i.e., deposition is dictated by the hydrodynamics and sediment transport of the jet only. Such early deposits are pivotal, because they likely determine what morphological feedback, either mouth bar or later levees, will develop in the future.

Potential vorticity (PV) or, equivalently, jet momentum are good indicators for the occurrence of mouth bars or lateral levees when the river mouth is deep and friction effects are negligible. Jets characterized by high PV tend to remain confined and deliver sediment to the margins, thus favoring the formation of levees [*Falcini et al*., 2014]. On the contrary, in shallow river mouths the main mechanism responsible for levee formation is jet instability, which is mostly controlled by bottom friction through the stability number S [*Canestrelli et al*., 2014].

In addition to autogenic sedimentary processes, waves can affect sediment redistribution between central and lateral deposits. The effect of waves depends on the scale at which the process is considered. At a short time scale, i.e., at the time scale of a single-channel formation, waves influence depositions by directly modifying the jet hydrodynamic. Waves increase the effective bed roughness [*Soulsby et al*., 1993] and jet spreading, thus shortening the distance at which the mouth bar is built [*Nardin et al*., 2013]. Wave-induced bed friction likely increases jet stability [*Canestrelli et al*., 2014], promoting mouth bar formation rather than levees.

Buoyancy seems to favor the formation of levees by producing flow convergence through the development of a paired of helical flow cells [*Wright and Coleman*, 1974], while tides facilitate the formation of mouth bars by increasing jet spreading and sediment deposition near the river mouth [*Leonardi et al*., 2013, 2014].

Incision underneath the jet is also important for promoting the formation of levees. *Chatanantavet and Lamb* [2014] show with a series of laboratory experiments that during high flow a drawdown river profile establishes near the mouth of the river, increasing water velocity and promoting erosion. This erosion augments water depth, leading to self-channelization of the jet and the construction of two lateral levees.

Reviews of Geophysics

10.1002/2014RG000451

Table 1. Processes Present at River Mouths and Their Effect on the Morphology of Mouth Deposits[a]

Process	Key Parameters	Morphological Effect on Mouth Deposits
Jet stability	Stability number S, Reynolds number Re_B	$S < S_c = 1.3\ 10^{-3} Re_B^{0.235}$ jet unstable, long lateral levees $S > S_c$, jet stable, mouth bar close to river mouth
Jet stability and jet momentum	Nondimensional jet momentum M Stability number S	Nondimensional mouth bar distance $L_B/B_0 = 0.17 + 0.58\ S + 0.08\ M$ Nondimensional levee length $L_L/B_0 = 0.71 + 0.87\ S + 0.07\ M$
Sediment eddy diffusivity (only unstable jets)	Deposition timescale $T_E = B_0/(0.07\ U)$ Large-eddy timescale $T_D = h/(2\ \omega_s)$	$T_E = T_D$ Optimal conditions for levees formation
Jet velocity	Ratio nondimensional bottom shear stress to Shields number τ^*/θ	$\tau^*/\theta < 1$ Sediment unable to exit river mouth
Tides (general)	Ratio river velocity to tidal velocity U_0/U_t, Tidal amplitude h_t	$(U_0\text{-}U_t)/(U_0 + U_t) < 0.34\text{–}1.3\ h_t/h$ central channel no mouth bar $(U_0\text{-}U_t)/(U_0 + U_t) < 0.34\text{–}1.3\ h_t/h$ Mouth bar
Tides (fluvial-dominated river mouth)	Tidal amplitude h_t	Wider and closer mouth bars (effect not quantified)
Waves (general)	Ratio between wave and river flow Bottom shear stresses P	$P > P_{cr}$ Absence of mouth bar and levees $P < P_{cr}$ Mouth bar and levees P_{cr} depends on wave angle at 0° (frontal waves) $P_{cr} = 0.9$, at 45° $P_{cr} = 0.18$
Waves (locally generated)	Significant wave height	Reduction of mouth bar distance (Figure 9b)
River mouth geometry	Width-to-depth ratio B_0/h	High width-to-depth ratio, high S, mouth bar close to river mouth
Sediment cohesion	Grain size D_{84}	High cohesion, low with-to-depth ratio (Figure 14), low S, long lateral levees
Friction	Friction factor c_f	High friction, high S, mouth bar close to river mouth

[a]The key parameters and available quantitative expressions are also indicated.

The importance of erosive processes in the extension of distributary channels and in the formation of lateral levees was also noticed in Wax Lake delta, Louisiana [*Shaw and Mohrig*, 2014]. During high flow, sand carried by the river accumulates both in the distributary channels and in foreset shoals. During low river flow, bed erosion is focused at the channel tips, with extension of the channel. Lateral levees form not only because of high deposition rates at the channel banks but also driven by channel incision [*Shaw and Mohrig*, 2014]. To summarize, the key processes and related parameters that affect river mouth deposits are reported in Table 1.

10. Implications for Delta Restoration and Erosion Mitigation Strategies

10.1. Rationale for Restoration

Recent research has documented the plight of river deltas around the world; in the face of land subsidence, rising sea level, reduced sediment supply, and increasing population density, many deltaic coastlines are retreating at a pace that is faster than coastal communities can adapt [*Britsch and Dunbar*, 1993; *Day et al*., 2000; *Penland et al*., 2005; *Georgiou et al*., 2005; *Syvitski and Saito*, 2007; *Campanella*, 2008; *Törnqvist et al*., 2008; *Syvitski et al*., 2009]. Land loss and inundation of river deltas is, at its core, a mass balance problem. For many large deltas, there is simply not enough sediment to maintain the current subaerial area and compensate for relative sea level rise. The canonical example is the Mississippi River Delta, USA, where coastal wetlands are disappearing at a rate of about 1% of land per year [*Britsch and Dunbar*, 1993; *Day et al*., 2000; *Penland et al*., 2005]. Extrapolating from current land loss rates, researchers have forecast that significant drowning of deltaic wetlands is inevitable [e.g., *Blum and Roberts*, 2009]. Here we will discuss the implications of research results on mouth bar deposits for delta restoration. However, it is important to highlight that the evolution of an entire delta includes many large-scale processes not included herein. River avulsion, with the abandonment of a river mouth and the creation of a new one, also affects sediment fluxes and land building [*Chatanantavet et al*., 2012; *Ganti et al*., 2014]. Waves affect the large-scale distribution of sediments near river mouths [*Bhattacharya and Giosan*, 2003; *Ashton and Giosan*, 2011] and sometimes produce barrier islands that help trapping sediments near the coast [*Giosan,* 2007]. Our analysis needs therefore to be integrated with studies on large-scale sediment transport processes in order to correctly assess the fate of an entire deltaic system.

While the shift in the mass balance equation on many deltas makes land loss inevitable, coastal erosion may be mitigated at judiciously selected sites through the construction of artificial diversions. On the Mississippi Delta, scientists, engineers, and managers have converged on restoration plans that involve the creation of artificial diversions to reconnect the river to deltaic wetlands [*DeLaune et al*., 2003; *Day et al*., 2007; *Kim et al*., 2009b; *Rego et al*., 2010; *Paola et al*., 2011; *Nittrouer et al*., 2012a; *Falcini et al*., 2012]. Some proposed plans aim to direct freshwater and sediment from the Mississippi River to shallower receiving basins to facilitate wetland growth in critical areas, including New Orleans' coastal buffer zone [*Kolker et al*., 2012]. Such diversions are expected to, in effect, build bars at their mouths. Much progress has been made in modeling the growth of mouth bars and river deltas due to artificial diversions. In particular, radially averaged (1-D) geometric models—based on mass conservation—predict realistic growth rates when applied to the Wax Lake (sub)Delta in the Mississippi system [see *Kim et al*., 2009b; *Paola et al*., 2011].

By their nature, however, such models cannot predict *how* growth will occur, as they explicitly assume radially symmetric growth. This growth pattern is indeed observed for the Wax Lake lobe of the Mississippi Delta, for example; but it is violated for the Birdsfoot Delta, which has created very elongated levees [cf. *Falcini and Jerolmack*, 2010]. For the purposes of building a land buffer, the geometry of Wax Lake is clearly preferable to the Birdsfoot. An analysis of the evolution of the Mississippi Delta during the Holocene indeed indicates that delta progradation occurred in different styles at different locations [*Roberts*, 1997].

Designing artificial diversions to produce prescribed growth patterns requires moving beyond a mass balance model to understand the mechanics of mass distribution. The next problem to solve in restoration sedimentology [cf. *Edmonds*, 2012] becomes how to distribute the limited sediment supply from impacted rivers in order to maximize land building potential. We consider three functions that artificial diversions should fulfill: (1) concentrate riverine sediment, (2) deliver it efficiently to a desired location, and (3) encourage deposition on wetlands and the nearshore environment. Below we consider how recent progress in our understanding of river mouth deposition informs our prospects of engineering restoration diversions.

10.2. The Mass Distribution Problem

One key aspect of the mass distribution problem is understanding the relative rates of mouth bar versus levee growth, which ultimately control the emergent geometry of the delta [*Falcini and Jerolmack*, 2010; *Edmonds and Slingerland*, 2010; *Mariotti et al*., 2013; *Falcini et al*., 2014; *Canestrelli et al*., 2014; *Caldwell and Edmonds*, 2014]. Research summarized in this paper shows two dominant controls: (1) river plume hydrodynamics and (2) sediment characteristics. Diffuse jets with rapid spreading encourage mouth bar deposition and flow divergence, reinforcing deposition of suspended sediment and resulting in the emergence of radially symmetric deltas. Focused jets that spread slowly may prevent mouth bar deposition while encouraging deposition at the jet margins, which further confines the flow and promotes the growth of elongated channels. These dynamics are well described by the stability number S and by the jet momentum (equivalent to PV) of the river plume [*Falcini and Jerolmack*, 2010; *Canestrelli et al*., 2014], and their consequences on river delta growth have been demonstrated with numerical simulations [*Canestrelli et al*., 2014]. The designed diversion should maximize stability parameter S, which control the location of the mouth bar. The jet stability can be increased by augmenting the diversion width, reducing the water depth, or increasing bottom friction in the receiving basin by adding, for example, artificial roughness (Table 1). Since the depth of the diversion needs to be equal to the depth of the river in order to allow bed load sediment transport, the diversion needs to be as large as possible to increase jet stability. At the same time the jet speed should be above the threshold of incipient transport for bed load (Table 1) in order to speed up the process of land building and avoid deposition of sediment in the diversion itself [*Canestrelli et al*., 2014]. As a result, the minimum Shields number for bed load transport ultimately controls the width of the diversion (Table 1).

Regarding sediment characteristics, both mass and cohesiveness are important. For noncohesive sediments, the Rouse number of the river plume is a key parameter. Coarse sediment such as sand, which is not well suspended by the jet, will deposit close to the river mouth, and promote mouth bar growth. Fine sediment such as silt, which is completely suspended by the jet, will disperse widely in a manner controlled by flow hydrodynamics. The interactions between sediment transport and unsteady coherent structures—large-scale horizontal eddies that detach from the flow at the river mouth—are also of paramount importance. In fact, sediments with a settling timescale comparable to the timescale of an eddy half rotation likely produce lateral levees [*Rowland et al*., 2010; *Mariotti et al*., 2013]. Since settling velocity of sand is a function of grain size, the large-scale coherent structures effectively determine what sediment characteristics are more prone to levees formation and should therefore be avoided in restoration projects. For instance, the settling velocity should be $\omega_s > 0.035\ Uh/B_0$ (see Table 1 and *Mariotti et al*. [2013]).

In terms of sediment cohesion, it is clear from numerical models [*Edmonds and Slingerland*, 2010] and field data [e.g., *Esposito et al*., 2013; *Nittrouer et al*., 2011] that it plays a role in the morphology of mouth deposits, but the exact mechanisms by which it acts are still unclear. It has been suggested that the large entrainment stress of fine sediments ($D_{50} < 63\ \mu$m) promotes levee growth, because fine sediment deposited at the margins of the jet cannot be eroded [*Edmonds and Slingerland*, 2010]. However, cohesion also influences the geometry of the feeder channel [*Caldwell and Edmonds*, 2014], making it narrower and deeper, which in turn produces unstable jets that promote levee deposition [*Canestrelli et al*., 2014; *Mariotti et al*., 2013].

A second key component of the mass distribution problem is the trapping efficiency of sediment within the delta [*Nardin and Edmonds*, 2014]. Only a fraction of the sediment load transported in a river is deposited on the delta plain, while the rest is delivered offshore and does not contribute to land building. In the presence of vegetation, up to 40% more sediment is trapped on the delta islands [*Nardin and Edmonds*, 2014]. Clearly, trapping efficiency is an important aspect of predicting delta growth rate into the basin. In geometric mass balance models the trapping efficiency is an input parameter [*Kim et al*., 2009b; *Paola et al*., 2011], but one would prefer that this efficiency is an emergent prediction from a model. Trapping efficiency depends strongly on the hydrodynamics of the river plume and its interactions with the ocean, which is controlled in part by the morphology of the river mouth. Observations during a flood on the Mississippi River Delta showed a relatively large sediment trapping efficiency associated with the high-friction jet issuing from the Atchafalaya/Wax Lake system. Importantly, sediments from this diffuse plume were trapped in the coastal zone for weeks, helping to promote marsh deposition. In contrast, there was a significantly lower trapping efficiency associated with the high-momentum jet emanating from the Birdsfoot Delta, which was observed to penetrate the coastal current and deliver sediment to the deep ocean [*Falcini et al*., 2012].

Predicting trapping efficiency will require a more refined understanding of the interaction of river plumes with the ocean, but its apparent relation to plume hydrodynamics suggests that the geometry of diversions may be tuned to optimize marsh and nearshore deposition. More research is needed to quantify the trapping efficiency or river mouths under different flow conditions.

One process that is often neglected in projects for delta restoration and erosion mitigation is the efficiency of the system in trapping fine-grained sediments (silt and clay). This component is often overlooked by the common emphasis on mouth bars. Trapping of fine sediments is dictated by the large-scale morphology and hydrodynamics of the shelf into which the river discharges. For example, shallow bays delimited by barrier islands are more adapted to sequester fine sediments [*Fagherazzi and Wiberg*, 2009]. Sediment depositions and resuspension in bays and estuaries is beyond the scope of this review, we refer to *Green and Coco* [2014] for a review of processing controlling the fate of sediments in these shallow environments.

10.3. Outlook

The above considerations provide a good starting place for designing restoration diversions under idealized conditions. Restoration is simplest, and the outcome most certain, for diversions into receiving waters with little wave or tide influence. Convergence of theory, experiment, numerical modeling, and field data give us great confidence in our ability to qualitatively and, to first-order, quantitatively predict land building as a result of initial and boundary conditions of a sediment-laden jet. The upshot is that stable jets produce the desired river mouth growth pattern and promote high sediment trapping efficiencies. Accordingly, diversions should be wide and shallow (largest width possible so that $\tau^*/\theta > 1$ with a depth equal to the river depth), conditions that enhance bottom friction and encourage mouth bar deposition [*Falcini and Jerolmack*, 2010; *Canestrelli et al*., 2014]. As noted by others, diversion structures should extract water from lower portions of the water column, where sediment concentrations are higher and sediment is coarser [*Paola et al*., 2011]. In addition, it may be possible to strategically select diversion sites that tap coarser sediments such as sand [e.g., *Edmonds and Slingerland*, 2010; *Nittrouer et al*., 2012a; *Caldwell and Edmonds*, 2014] to further promote mouth bar deposition. Using a target value for the jet momentum and stability parameter, numerical simulations of delta growth from designed diversions may be undertaken to predict growth rates [*Canestrelli et al*., 2014]. The geometry of the diversion mouth can be also designed to maximize sediment eddy diffusivity, based on knowledge of sediment characteristics and large-scale eddy dynamics [*Mariotti et al*., 2013].

Of course, there are myriad factors that complicate the above picture; we consider a few outstanding ones here. As discussed in this paper, waves and tides exert a strong influence on the spreading of river mouth jets. Waves may suppress mouth bar formation or change the direction of progradation, resulting in large-scale differences in delta morphology that have been explored in numerical experiments [*Nardin and Fagherazzi*, 2012; *Nardin et al*., 2013]. Locally generated waves with short period help stabilizing the jet, favoring deposition near the river mouth [*Nardin et al*., 2013]. Less explored is the effect of waves on sediment trapping efficiency in the delta. Long-shore drift resulting from the wavefield may remove sediments from the river mouth and deposit them far downshore, potentially reducing delta trapping efficiency compared to a wave-free situation. However, feedbacks between long-shore sediment transport and river discharge can produce complex nonlinear dynamics. For example, in the Danube Delta, Romania, the river plume acts as a groin-reducing wave energy thus producing a shoaling effect in the downdrift area. As a result, sequestration of sediments occurs near the river mouth [*Giosan,* 2007]. The morphologic effect of tides has also been demonstrated in numerical simulations [*Leonardi et al*., 2013, 2014]. Tides increase jet spreading and lead to a faster bar aggradation but, again, the influence on sediment trapping efficiency is largely unknown. Our review has not considered the influence of large-scale marine processes such as coastal currents, mainly because simulations are only now beginning to capture the interactions of river plumes with a truly dynamic ocean [e.g., *Rego et al*., 2010; *Kourafalou and Androulidakis*, 2013]. These dynamics may have an important but, as yet unknown, influence on land building from diversions by influencing sediment trapping efficiency and/or shallow shelf sedimentation.

Besides marine processes, another difficulty lies in understanding the generation of organic matter in river mouth deposits. The processes we have discussed thus far control the deposition rates of mineral (nonorganic) riverine sediment. However, organic matter is often a significant fraction of the composition of a river delta; it is anywhere from 10% to 40% by weight for the Mississippi Delta coastal marshes, for

example [*Lorenzo-Trueba et al*., 2012; *Khan et al*., 2013]. Biological drivers of sediment accumulation are beyond the scope of this review. However, it is likely that organic matter accumulation affects a quantitative change in the mass balance, but not a qualitative change in river mouth dynamics. Mineral sediment must build the subaqueous levees or bars up to (or close to) the sea surface; only when land becomes emergent can vegetation take hold and begin generating organic matter. Accordingly there is hope that, as our understanding of the controls on organic matter accumulation rate increases, a simple submodel for this process may be added to numerical models of river mouth deposits. A better understanding of the processes controlling organic matter accumulation could aid in restoration; a diversion could provide a "bigger bang for the buck" if mineral sedimentation patterns could be tuned to optimize organic matter accumulation. Besides influencing organic matter generation, vegetation likely exerts additional controls on river mouth deposition and morphology through the binding power of its roots, as discussed earlier in this review. As in other areas of geomorphology, understanding biophysical processes and feedbacks is a frontier topic in river delta research.

The results reported here show that high-resolution numerical models, like Delft3D, have the capability to simulate in detail the deposition of sediments at river mouths. On the contrary, 1-D models cannot capture complex dynamics like the spreading of the jet exiting the river mouth or the formation of large eddies due to flow instability. More research is, however, needed to capture all the processes responsible for sediment trapping in these environments.

11. Future Research Needs

Surprisingly, lunate bars [*Bates* 1953] and the processes that form them have received little attention in recent years: more research is needed to determine under what conditions they form at river mouths. Similarly, the effect of buoyancy and internal waves on the deposition of sediments at river mouths has not been the focus of recent investigations.

An important component in the evolution or river mouth deposits is the suite of processes that increase aggradation on bars and levees until they become emergent. Halophytic vegetation is a key player in the transition between submerged and emerged landforms, and more research is needed to understand this critical phase. Some key results and processes can be borrowed by the wealth of data collected in salt marshes, which are located at similar elevations within the tidal range and capture large volumes of coastal sediments (see *Fagherazzi et al*. [2012] for a review). However, deltaic and river mouth islands might present unique ecological and geomorphological feedbacks, due to the presence of freshwater vegetation and intermittent sediment delivery [e.g., *Nardin and Edmonds*, 2014]. More research is also needed to understand how several subaqueous bars and levees and their subaerial equivalents interact with each other to form the overall architecture and morphology of deltas (see Figure 1).

Several of the results presented herein suggest possible strategies on how to maximize sediment deposition at river mouths in order to build new land. Unfortunately, many of these results are qualitative and limited in nature, without exploring the full range of river mouth configurations and flow conditions. A quantitative analysis of all factors affecting the total volume of sediments deposited at river mouths is much needed and would help restoration and mitigation projects at the shoreline.

Several of the results presented herein are based on a steady flow of water and sediments exiting a river mouth. This hydrodynamic simplification neglects the typical unsteadiness of rivers, which carry most of the water and sediment during relatively infrequent floods. Field measurements and numerical modeling of the lowermost portion of the Mississippi River show that during low flow a backwater surface profile establishes leading to low flow velocities and sediment deposition [*Nittrouer et al*., 2011; *Lamb et al*., 2012]. During high flow, the surface water switches to a drawdown profile that accelerates flow producing localized scour near the river mouth [*Nittrouer et al*., 2011; *Lamb et al*., 2012]. As a result, both the river mouth morphology and patterns of sediment delivery to the ocean are strongly affected by nonuniform flow conditions linked to the river hydrograph [*Nittrouer et al*., 2012b; *Lamb et al*., 2012]. Future research will have to account for the variability in discharge and sediment load at river mouths, thus integrating in a unique framework the lower reaches of a river and its mouth deposits.

The role of vegetation on sediment dynamics at river mouths needs also to be addressed in more detail. Vegetation is the key element during the transition from subaqueous mouth bars and levees to stable subaerial islands and thus controls the final size and geometry of sediment deposits. We are only beginning to understand how vegetation affects sediment transport at river mouths [e.g., *Nardin and Edmonds*, 2014]. More research is clearly needed to quantify all the feedbacks between biology and geomorphology.

Nomenclature

A	asymmetry index (net long-shore transport rate divided by river discharge)
a	dynamic expansion coefficient (m^{-1})
$\overline{b} = b/b_0$	dimensionless half width of the jet (m)
$b(x)$	local half width of the expanding jet (m)
b_0	half width of river mouth (m)
B_0	width of river mouth (m)
c_f	friction factor in the formulation $\tau = \rho U^2 c_f/2$, with τ the bottom shear stress
$C = \sqrt{2g/c_f}$	Chezy coefficient ($m^{1/2}/s$)
D_{50}	median grain diameter (m)
f_w	waves friction coefficient
g	acceleration due to gravity (m/s^2)
h	water depth (m)
h'	thickness of the plume (m)
H_S	significant wave height (m)
h_t	tidal amplitude (m)
$\hat{h}_v$	vegetation height relative to average flow depth
I_1, I_2	space integrals in Ozsoy jet theory
K	wave number (m^{-1})
L_{RMB}	distance to river mouth bar (m)
L_{RMBW}	distance to river mouth bar in the presence of waves (m)
m	ratio between combined wave-current bottom shear stress and current shear stress
P	ratio of the wave shear stress and the current shear stress at the river mouth
Q	flow discharge at the river mouth (m^3/s)
Re_{B}	Reynolds number, with B as length scale
Re_{h}	Reynolds number, with h as length scale
R_w	ratio of water fluxes on vegetated bar surfaces relative to nonvegetated conditions
S	stability number
S_c	critical stability number
T_D	deposition time scale (s)
T_E	large-eddy time scale (s)
T_P	peak period (s)
u	streamwise velocity (m/s)
U	jet-averaged velocity magnitude (m/s)
U_0	velocity at the inlet (m/s)
u_b	wave bottom orbital velocity (m/s)
u_c	centerline velocity (m/s)
$\overline{u} = u/U_0$	dimensionless velocity at the jet centerline
U_e	rate of entrainment into the discharging effluent (m/s)
U_t	tidal velocity (m/s)
w_s	grain settling velocity (m/s)
W	ratio between wave and river flow bottom shear stresses
W_{cr}	critical value of W for the formation of mouth deposits
x	dimensional longitudinal coordinate (m)
x_s, ξ_s	location of transition between ZOFE and ZOEF
τ_*	nondimensional bottom shear stress

τ_c	current bottom shear stress ($kg\,m^{-1}\,s^{-2}$)
τ_m	combined wave-current bottom shear stress ($kg\,m^{-1}\,s^{-2}$)
τ_w	waves bottom shear stress ($kg\,m^{-1}\,s^{-2}$)
α	entrainment rate of the jet
γ	relative density of the outflow
θ	Shields number
Φ	wave angle with respect to shore normal (°)
η	dimensionless coordinate perpendicular to the jet centerline
ν	molecular viscosity ($kg\,s^{-1}\,m^{-1}$)
ν_T	turbulent viscosity ($kg\,s^{-1}\,m^{-1}$)
ρ	fluid density ($kg\,m^{-3}$)
ρ_f	fluid density of the outflow ($kg\,m^{-3}$)
ρ_s	fluid density of the receiving water ($kg\,m^{-3}$)
σ	density of quartz ($kg\,m^{-3}$)
$\xi = x/b_0$	nondimensional longitudinal coordinate
ω_s	sediment settling velocity

Acknowledgments

S.F. was supported by Exxon Mobil Upstream Research Company award EM01830, the ACS-PRF program award 51128-ND8, and by NSF award OCE-0948213. R.S. was supported by NSF grants EAR-0417877, OCE-1061495, and NSF 10-577. D.A.E. was supported by NSF grants FESD/EAR-1135427 and OCE-1061380. The data used in this review were derived from publications found in the Reference List.

Gregory Okin was the Editor for this manuscript. He thanks Jeffrey Nittrouer, Andrew Ashton, and three anonymous reviewers for their assistance in reviewing this manuscript.

References

Abramovich, G. N. (1963), *Theory of Turbulent Jets*, MIT Press, Cambridge, Mass.

Albertson, M. L., Y. B. Dai, R. A. Jensen, and H. Rouse (1950), Diffusion of submerged jets, *Trans. Am. Soc. Civil Eng.*, *115*, 639–664.

Ashton, A. D., and L. Giosan (2011), Wave-angle control of delta evolution, *Geophys. Res. Lett.*, *38*, L13405, doi:10.1029/2011GL047630.

Axelsson, V. (1967), The Laitaure Delta: A study of deltaic morphology and processes, *Geogr. Ann. Ser. A: Phys. Geogr.*, *49*(1), 127.

Baptist, M. (2005), Modelling floodplain biogeomorphology, PhD thesis, Delft Univ. Press, Delft, Netherlands.

Batchelor, G. K. (1969), Computation of the energy spectrum in homogeneous two-dimensional turbulence, *Phys. Fluids Suppl II*, *12*, 233–239.

Bates, C. C. (1953), Rational theory of delta formation, *AAPG Bull.*, *37*(9), 2119–2162.

Bhattacharya, J. P., and L. Giosan (2003), Wave-influenced deltas: Geomorphological implications for facies reconstruction, *Sedimentology*, *50*, 187–210.

Black, K. S., T. J. Tolhurst, D. M. Paterson, and S. E. Hagerthey (2002), Working with natural cohesive sediments, *J. Hydraul. Eng.*, *128*, 2–8.

Blum, M. D., and H. H. Roberts (2009), Drowning of the Mississippi Delta due to insufficient sediment supply and global sea-level rise, *Nat. Geosci.*, *2*, 488–491.

Bondar, C. (1970), Considerations théoriques sur la dispersion d'un courant liquide de densité réduite et à niveau libre, dans un bassin contenant un liquide d'une plus grande densité, in *Proceedings Symposium on the Hydrology of Deltas*, *AISH Publ.*, vol. 11, pp. 246–256, Unesco, Paris.

Bonham-Carter, G., and A. J. Sutherland (1968), *Mathematical Model and Fortran IV Program for Computer Simulation of Deltaic Sedimentation*, *Kansas Geol. Surv. Comp. Contrib. 24*, 56 pp., Univ. of Kans., Lawrence.

Bonham-Carter, G. F., and A. J. Sutherland (1967), Diffusion and settling of sediments at river mouths: A computer simulation model, *Trans. Gulf Coast Assoc. Geol. Soc.*, *17*, 326–338.

Booij, N., R. C. Ris, and L. H. Holthuijsen (1999), A third-generation wave model for coastal regions: 1. Model description and validation, *J. Geophys. Res.*, *104*(C4), 7649–7666.

Borichansky, L. S., and V. N. Mikhailov (1966), Interaction of river and sea water in the absence of tides, in *Scientific Problems of the Humid Tropical Zone Deltas and Their Implications*, pp. 175–180, UNESCO Publ. Center, New York.

Bradbury, L. J. (1965), Structure of a self-preserving turbulent plane jet, *J. Fluid Mech.*, *23*(1), 31.

Bridge, J. S. (2003), *Rivers and Floodplains: Forms, Processes, and Sedimentary Record*, Blackwell, Malden, Mass.

Britsch, L. D., and J. B. Dunbar (1993), Land loss rates: Louisiana coastal plain, *J. Coastal Res.*, *9*, 324–338.

Caldwell, R. L., and D. A. Edmonds (2014), The effects of sediment properties on deltaic processes and morphologies: A numerical modeling study, *J. Geophys. Res. Earth Surf.*, *119*, 961–982.

Cai, H., H. H. G. Savenije, and M. Toffolon (2013), Linking the river to the estuary: Influence of river discharge on tidal damping, *Hydrol. Earth Syst. Sci. Discuss.*, *10*(7), 9191–9238, doi:10.5194/hessd-10-9191-2013.

Campanella, R. (2008), *Bienville's Dilemma: A Historical Geography of New Orleans*, 429 pp., Univ. of La., Lafayette.

Camporeale, C., E. Perucca, L. Ridolfi, and A. M. Gurnell (2013), Modeling the interactions between river morphodynamics and riparian vegetation, *Rev. Geophys.*, *51*, 379–414, doi:10.1002/rog.20014.

Canestrelli, A., W. Nardin, D. Edmonds, S. Fagherazzi, and R. Slingerland (2014), Importance of frictional effects and jet instability on the morphodynamics of river mouth bars and levees, *J. Geophys. Res. Oceans*, *119*, 509–522, doi:10.1002/2013JC009312.

Chatanantavet, P., and M. P. Lamb (2014), Sediment transport and topographic evolution of a coupled river and river-plume system: An experimental and numerical study, *J. Geophys. Res. Earth Surf.*, *119*, 1263–1282, doi:10.1002/2013JF002810.

Chatanantavet, P., M. P. Lamb, and J. A. Nittrouer (2012), Backwater controls of avulsion location on deltas, *Geophys. Res. Lett.*, *39*, L01402, doi:10.1029/2011GL050197.

Chen, D., and G. H. Jirka (1998), Linear stability analysis of turbulent mixing layers and jets in shallow water layers, *J. Hydraul. Res.*, *36*, 815–830.

Costanza, R., O. Pérez-Maqueo, M. L. Martinez, P. Sutton, S. J. Anderson, and K. Mulder (2008), The value of coastal wetlands for hurricane protection, *AMBIO: A J. Human Environ.*, *37*(4), 241–248.

D'Alpaos, A., S. Lanzoni, M. Marani, and A. Rinaldo (2010), On the tidal prism-channel area relations, *J. Geophys. Res.*, *115*, F01003, doi:10.1029/2008JF001243.

Dalrymple, R. W., and K. Choi (2007), Morphologic and facies trends through the fluvial–marine transition in tide-dominated depositional systems: A schematic framework for environmental and sequence-stratigraphic interpretation, *Earth Sci. Rev.*, *81*(3–4), 135–174.

Dalrymple, R. W., E. K. Baker, P. T. Harris, and M. Hughes (2003), Sedimentology and stratigraphy of a tide-dominated, foreland-basin delta (Fly River, Papua New Guinea), *SEPM Spec. Publ*, *76*, 147–173.
Day, J. W., L. D. Britsch, S. R. Hawes, G. P. Shaffer, D. J. Reed, and D. Cahoon (2000), Pattern and process of land loss in the Mississippi Delta: A spatial and temporal analysis of wetland habitat change, *Estuaries*, *23*(4), 425–438.
Day, G., W. E. Dietrich, J. C. Rowland, and A. Marshall (2008), The depositional web on the floodplain of the Fly River, Papua New Guinea, *J. Geophys. Res.*, *113*, F01S02, doi:10.1029/2006JF000622.
Day, J. W., et al. (2007), Restoration of the Mississippi Delta: Lessons from Hurricanes Katrina and Rita, *Science*, *315*, 1679–1684.
de Swart, H. E., and J. T. F. Zimmerman (2009), Morphodynamics of tidal inlet systems, *Annu. Rev. Fluid Mech.*, *41*, 203–229.
DeLaune, R. D., A. Jugsujinda, G. W. Peterson, and W. H. Patrick (2003), Impact of Mississippi River freshwater reintroduction on enhancing marsh accretionary processes in a Louisiana estuary, *Estuarine Coastal Shelf Sci.*, *58*, 653–662.
Dracos, T., M. Giger, and G. H. Jirka (1992), Plane turbulent jets in a bounded fluid layer, *J. Fluid Mech.*, *241*, 587–614.
DuMars, A. J. (2002), Distributary mouth bar formation and channel bifurcation in the Wax Lake Delta, Atchafalaya Bay, in *Louisiana Geology and Geophysics*, 88 pp., Master of Sci., La. State Univ., Baton Rouge.
Edmonds, D. A. (2012), Restoration sedimentology, *Nat. Geosci.*, *5*, 758–759, doi:10.1038/ngeo1620.
Edmonds, D. A., and R. L. Slingerland (2007), Mechanics of river mouth bar formation: Implications for the morphodynamics of delta distributary networks, *J. Geophys. Res.*, *112*, F02034, doi:10.1029/2006JF000574.
Edmonds, D. A., and R. L. Slingerland (2008), Stability of delta distributary networks and their bifurcations, *Water Resour. Res.*, *44* W09426, doi:10.1029/2008WR006992.
Edmonds, D. A., and R. L. Slingerland (2010), Significant effect of sediment cohesion on delta morphology, *Nat. Geosci.*, *3*(2), 105–109.
Edmonds, D. A., D. C. J. D. Hoyal, B. A. Sheets, and R. L. Slingerland (2009), Predicting delta avulsions: Implications for coastal wetland restoration, *Geology*, *37*(8), 759–762.
Edmonds, D. A., J. B. Shaw, and D. Mohrig (2011), Topset-dominated deltas: A new model for river delta stratigraphy, *Geology*, *39*(12), 1175–1178.
Ertel, H. (1942), Einneuerhydrodynamischer Wirbelsatz, *Meteorol. Z.*, *59*(2), 277–281.
Esposito, C. R., I. Y. Georgiou, and A. S. Kolker (2013), Hydrodynamic and geomorphic controls on mouth bar evolution, *Geophys. Res. Lett.*, *40*, 1540–1545, doi:10.1002/grl.50333.
Everitt, K. W., and A. G. Robins (1978), Development and structure of turbulent plane jets, *J. Fluid Mech.*, *88*, 563–583.
Fagherazzi, S., and I. Overeem (2007), Models of deltaic and inner continental shelf landform evolution, *Annu. Rev. Earth Planet. Sci.*, *35*, 685–715.
Fagherazzi, S., and P. L. Wiberg (2009), Importance of wind conditions, fetch, and water levels on wave-generated shear stresses in shallow intertidal basins, *J. Geophys. Res.*, *114*, F03022, doi:10.1029/2008JF001139.
Fagherazzi, S., M. L. Kirwan, S. M. Mudd, G. R. Guntenspergen, S. Temmerman, A. D'Alpaos, J. Koppel, J. M. Rybczyk, E. Reyes, and C. Craft (2012), Numerical models of salt marsh evolution: Ecological, geomorphic, and climatic factors, *Rev. Geophys.*, *50*, RG1002, doi:10.1029/2011RG000359.
Falcini, F., and D. J. Jerolmack (2010), A potential vorticity theory for the formation of elongate channels in river deltas and lakes, *J. Geophys. Res.*, *115*, F04038, doi:10.1029/2010JF001802.
Falcini, F., et al. (2012), Linking the historic 2011 Mississippi River flood to coastal wetland sedimentation, *Nat. Geosci.*, *5*, 803–807, doi:10.1038/ngeo1615.
Falcini, F., A. Piliouras, R. Garra, A. Guerin, D. J. Jerolmack, J. Rowland, and C. Paola (2014), Hydrodynamic and suspended sediment transport controls on river mouth morphology, *J. Geophys. Res. Earth Surf.*, *119*, 1–11, doi:10.1002/2013JF002831.
Farmer, R. C., and W. R. Waldrop (1977), A model for sediment transport and delta formation, *Waterway. Port Coastal Ocean Div. Am. Soc. Civ. Eng.*, *5*, 102–115.
Fischer, H. B. (1973), Longitudinal dispersion and turbulent mixing in open-channel flow, *Annu. Rev. Fluid Mech.*, *5*, 59–78.
Fitzgerald, D. M. (1996), Geomorphic variability and morphologic and sedimentologic controls on tidal inlets, *J. Coastal Res., Spec*, *23*, 47–72, doi:10.2307/25736068.
FitzGerald, D. M., I. Buynevich, and B. Argow (2006), Model of tidal inlet and barrier island dynamics in a regime of accelerated sea level rise, *J. Coastal Res.*, *39*, 789–795, doi:10.2307/25741684.
Foss, J. F., and J. B. Jones (1968), Secondary flow effects in a bounded rectangular jet, *J. Basic Eng.*, *9*(2), 241–248.
Ganti, V., Z. Chu, M. P. Lamb, J. A. Nittrouer, and G. Parker (2014), Testing morphodynamic controls on the location and frequency of river avulsions on fans versus deltas: Huanghe (Yellow River), China, *Geophys. Res. Lett.*, *41*, 7882–7890, doi:10.1002/2014GL061918.
Geleynse, N., J. E. A. Storms, M. J. F. Stive, H. R. A. Jagers, and D. J. R. Walstra (2010), Modeling of a mixed-load fluvio-deltaic system, *Geophys. Res. Lett.*, *37*, L05402, doi:10.1029/2009GL042000.
Geleynse, N., J. E. A. Storms, D. J. R. Walstra, H. Jagers, Z. B. Wang, and M. J. F. Stive (2011), Controls on river delta formation; insights from numerical modelling, *Earth Planet. Sci. Lett.*, *302*(1–2), 217–226.
Gelfenbaum, G., A. Stevens, E. Elias, and J. Warrick (2009), Modeling sediment transport and delta morphology on the dammed Elwha River, Washington State, USA, in *Proceedings Coastal Dynamics 2009*, 109 pp., World Sci. Group, London.
Georgiou, I. Y., D. M. FitzGerald, and G. W. Stone (2005), The impact of physical processes along the Louisiana coast, *J. Coastal Res.*, *44*, 72–89.
Giger, M., T. Dracos, and G. H. Jirka (1991), Entrainment and mixing in plane turbulent jets in shallow-water, *J. Hydraul. Res.*, *29*(5), 615–642.
Giosan, L. (2007) Morphodynamic feedbacks on deltaic coasts: Lessons from the wave-dominated Danube Delta, in *Coastal Sediments '07*, pp. 828–841, Am. Soc. of Civil Eng., Reston, Va., doi:10.1061/40926(239)63.
Goldschmidt, V. W., and M. F. Young (1975), Energy spectrum and turbulent scales in a plane air jet, in *Proceedings of 4th Biennial Symposium on Turbulent in Liquids*, 39 pp., Rolla-Missouri, Rolla, Mo.
Gosselink, J., and E. C. Pendleton (1984), *The Ecology of Delta Marshes of Coastal Louisiana: A Community Profile*, Louisiana State Univ Baton Rouge Center For Wetland Resources, Washington, D. C.
Green, M. O., and G. Coco (2014), Review of wave-driven sediment resuspension and transport in estuaries, *Rev. Geophys.*, *52*, 77–117, doi:10.1002/2013RG000437.
Hayes, M. O. (1980), General morphology and sediment patterns in tidal inlets, *Sediment. Geol.*, *26*(1), 139–156.
Hey, R. D., and C. R. Thorne (1986), Stable channels with mobile gravel beds, *J. Hydraul. Eng.*, *112*(8), 671–689.
Holdeman, J. D., and J. F. Foss (1975), Initiation, development, and decay of secondary flow in a bounded jet, *J. Fluids Eng. Trans. Asme*, *97*(3), 342–352.
Horner-Devine, A. R. (2009), The bulge circulation in the Columbia River plume, *Cont. Shelf Res.*, *29*(1), 234–251.
Hoyal, D. C. J. D., and B. A. Sheets (2009), Morphodynamic evolution of experimental cohesive deltas, *J. Geophys. Res.*, *114*, F02009, doi:10.1029/2007JF000882.

Huang, H. Q., and G. C. Nanson (1997), Vegetation and channel variation: A case study of four small streams in southeastern Australia, *Geomorphology*, *18*, 237–249.
Izumi, N., M. Date, and H. Tanaka (1999), Inceptive topography of fluvial-dominated river mouth bars, in *River Sedimentation: Theory and Applications*, *Seventh Int. Symp. on River Sediment*., pp. 899–904, Balkema, Rotterdam.
Jerolmack, D. J., and C. Paola (2007), Complexity in a cellular model of river avulsion, *Geomorphology*, *91*(3–4), 259–270.
Jerolmack, D. J., and J. Swenson (2007), Scaling relationships and evolution of distributary networks on wave-influenced deltas, *Geophys. Res. Lett.*, *34*, L23402, doi:10.1029/2007GL031823.
Jirka, G. H. (1994), Shallow jets, in *Recent Research Advances in the Fluid Mechanics of Turbulent Jets and Plumes*, edited by P. A. Davies and M. J. Valente Neves, pp. 155–175, Kluwer Acad., Dordrecht, Netherlands.
Jirka, G. H. (2001), Large scale flow structures and mixing processes in shallow flows, *J. Hydraul. Res.*, *39*(6), 567–573.
Johnson, W., C. Sasser, and J. Gosselink (1985), Succession of vegetation in an evolving river delta, Atchafalaya Bay, Louisiana, *J. Ecol.*, *73*, 973–986.
Jopling, H. (1963), Hydraulic studies on the origins of bedding, *Sedimentology*, *2*, 115–121.
Khan, N. S., B. P. Horton, K. L. McKee, D. Jerolmack, F. Falcini, M. D. Enache, and C. H. Vane (2013), Tracking sedimentation from the historic AD 2011 Mississippi River flood in the deltaic wetlands of Louisiana, USA, *Geology*, *41*(4), 391–394.
Kim, W. (2012), GEOMORPHOLOGY: Flood-built land, *Nat. Geosci.*, *5*(8), 521–522.
Kim, W., A. Dai, T. Muto, and G. Parker (2009a), Delta progradation driven by an advancing sediment source: Coupled theory and experiment describing the evolution of elongated deltas, *Water Resour. Res.*, *45*, W06428, doi:10.1029/2008WR007382.
Kim, W., D. Mohrig, R. Twilley, C. Paola, and G. Parker (2009b), Is it feasible to build new land in the Mississippi River delta?, *Eos Trans. AGU*, *90*(42), 373–374, doi:10.1029/2009EO420001.
Kolker, A. S., M. D. Miner, and H. D. Weathers (2012), Depositional dynamics in a river diversion receiving basin: The case of the West Bay Mississippi River Diversion, *Estuarine Coastal Shelf Sci.*, *106*, 1–12.
Kourafalou, V. H., and Y. S. Androulidakis (2013), Influence of Mississippi River induced circulation on the Deepwater Horizon oil spill transport 118, *J. Geophys. Res. Oceans*, *118*, 3823–3842, doi:10.1002/jgrc.20272.
Kundu, P. K., I. M. Cohen, and D. R. Dowling (2011), *Fluid Mechanics*, 5th ed., Academic Press, Waltham, Mass.
Lamb, M. P., J. A. Nittrouer, D. Mohrig, and J. Shaw (2012), Backwater and river plume controls on scour upstream of river mouths: Implications for fluvio-deltaic morphodynamics, *J. Geophys. Res.*, *117*, F01002, doi:10.1029/2011JF002079.
Landel, J. R., C. P. Caulfield, and A. W. Woods (2012), Meandering due to large eddies and the statistically self-similar dynamics of quasi-two-dimensional jets, *J. Fluid Mech.*, *692*, 347–368.
Lanzoni, S., and G. Seminara (1998), On tide propagation in convergent estuaries, *J. Geophys. Res.*, *103*(C13), 30,793–30,812, doi:10.1029/1998JC900015.
Leonardi, N., A. Canestrelli, T. Sun, and S. Fagherazzi (2013), Effect of tides on mouth bar morphology and hydrodynamics, *J. Geophys. Res. Oceans*, *118*, 4169–4183, doi:10.1002/jgrc.20302.
Leonardi, N., T. Sun, and S. Fagherazzi (2014), Modeling tidal bedding in distributary mouth bars, *J. Sediment. Res.*, *84*(6), 499–512.
Lesser, G. R., J. A. Roelvink, J. A. T. M. van Kester, and G. S. Stelling (2004), Development and validation of a three-dimensional morphological model, *Coastal Eng.*, *51*(8–9), 883–915.
Lorenzo-Trueba, J., V. R. Voller, C. Paola, R. R. Twilley, and A. E. Bevington (2012), Exploring the role of organic matter accumulation on delta evolution, *J. Geophys. Res.*, *117*, F00A02, doi:10.1029/2012JF002339.
Mariotti, G., F. Falcini, N. Geleynse, M. Guala, T. Sun, and S. Fagherazzi (2013), Sediment eddy diffusivity in meandering turbulent jets: Implications for levee formation at river mouths, *J. Geophys. Res. Earth Surf.*, *118*, 1908–1920, doi:10.1002/jgrf.20134.
Mikhailov, V. N. (1966), Hydrology and formation of river-mouth bars, in *Scientific Problems of the Humid Tropical Zone Deltas and Their Implications*, vol. 1, pp. 59–64, United Nations Educational, Scientific and Cultural Organization, Paris.
Mudd, S. M., S. M. Howell, and J. T. Morris (2010), Impact of dynamic feedbacks between sedimentation, sea-level rise, and biomass production on near-surface marsh stratigraphy and carbon accumulation, *Estuarine Coastal Shelf Sci.*, *82*(3), 377–389.
Nardin, W., and D. A. Edmonds (2014), Optimum vegetation height and density for inorganic sedimentation in deltaic marshes, *Nat. Geosci.*, *7*(10), 722–726.
Nardin, W., and S. Fagherazzi (2012), The effect of wind waves on the development of river mouth bars, *Geophys. Res. Lett.*, *39*, L12607, doi:10.1029/2012GL051788.
Nardin, W., G. Mariotti, D. A. Edmonds, R. Guercio, and S. Fagherazzi (2013), Growth of river mouth bars in sheltered bays in the presence of frontal waves, *J. Geophys. Res. Earth Surf.*, *118*, 872–886, doi:10.1002/jgrf.20057.
Nepf, H. M. (1999), Drag, turbulence, and diffusion in flow through emergent vegetation, *Water Resour. Res.*, *35*(2), 479–489.
Nicholls, R. J., and N. Mimura (1998), Regional issues raised by sea-level rise and their policy implications, *Clim. Res.*, *11*(1), 5–18.
Nittrouer, J. A., D. Mohrig, M. A. Allison, and A. P. B. Peyret (2011), The lowermost Mississippi River: A mixed bedrock-alluvial channel, *Sedimentology*, *58*(7), 1914–1934.
Nittrouer, J. A., J. L. Best, C. Brantley, R. W. Cash, M. Czapiga, P. Kumar, and G. Parker (2012a), Mitigating land loss in coastal Louisiana by controlled diversion of Mississippi River sand, *Nat. Geosci.*, *5*, 534–537, doi:10.1038/ngeo1525.
Nittrouer, J. A., J. Shaw, M. P. Lamb, and D. Mohrig (2012b), Spatial and temporal trends for water-flow velocity and bed-material sediment transport in the lower Mississippi River, *Geol. Soc. Am. Bull.*, *124*(3–4), 400–414.
Orton, G. J., and H. G. Reading (1993), Variability of deltaic processes in terms of sediment supply, with particular emphasis on grain size, *Sedimentology*, *40*, 475–512.
Overeem, I., J. P. M. Syvitski, and E. W. H. Hutton (2005), Three-dimensional numerical modeling of deltas, in *River Deltas: Concepts, Models and Examples*, *SEPM Spec. Publ.*, edited by J. P. Bhattacharya and L. Giosan, 83 pp., 13–30, SEPM, Tulsa, Okla.
Ozsoy, E. (1977), Flow and mass transport in the vicinity of tidal inlets, *Tech. Rep. TR-026*, Coastal and Oceanogr. Eng. Lab., Univ. of Fla., Gainesville.
Ozsoy, E., and U. Unluata (1982), Ebb-tidal flow characteristics near inlets, *Estuarine Coastal Shelf Sci.*, *14*(3), 251–263.
Paola, C., R. R. Twilley, D. A. Edmonds, W. Kim, D. Mohrig, G. Parker, E. Viparelli, and V. R. Voller (2011), Natural processes in delta restoration: Application to the Mississippi Delta, *Annu. Rev. Mar. Sci.*, *3*, 67–91, doi:10.1146/annurev-marine-120709-142856.
Pedlosky, J. (1987), *Geophysical Fluid Dynamics*, Springer, New York.
Penland, S., P. F. Connor, A. Beall, S. Fearnley, and S. J. Williams (2005), Changes in Louisiana's shoreline: 1855–2002, *J. Coastal Res.*, *44*, 7–39.
Ramaprian, B. R., and M. S. Chandrasekhara (1985), LDA measurements in plane turbulent jets, *J. Fluids Eng. Trans. ASME*, *107*(2), 264–271.
Rego, J. L., E. Meselhe, J. Stronach, and E. Habib (2010), Numerical modeling of the Mississippi-Atchafalaya Rivers' sediment transport and fate: Considerations for diversion scenarios, *J. Coastal Res.*, *26*(2), 212–229, doi:10.2112/08-1072.1.
Roberts, H. H. (1997), Dynamic changes of the Holocene Mississippi River delta plain: The delta cycle, *J. Coastal Res.*, *13*(3), 605–627.

Roelvink, J. A., and G. Van Banning (1994), Design and development of DELFT3D and application to coastal morphodynamics, *Hydroinformatics*, *94*, 451–455.
Rosen, T., and Y. J. Xu (2013), Recent decadal growth of the Atchafalaya River Delta complex: Effects of variable riverine sediment input and vegetation succession, *Geomorphology*, *194*, 108–120.
Rowland, J. C., M. T. Stacey, and W. E. Dietrich (2009a), Turbulent characteristics of a shallow wall-bounded plane jet: Experimental implications for river mouth hydrodynamics, *J. Fluid Mech.*, *627*, 423–449, doi:10.1017/S0022112009006107.
Rowland, J. C., W. E. Dietrich, G. Day, and G. Parker (2009b), Formation and maintenance of single-thread tie channels entering floodplain lakes: Observations from three diverse river systems, *J. Geophys. Res.*, *114*, F02013, doi:10.1029/2008JF001073.
Rowland, J. C., W. E. Dietrich, and M. T. Stacey (2010), Morphodynamics of subaqueous levee formation: Insights into river mouth morphologies arising from experiments, *J. Geophys. Res.*, *115*, F04007, doi:10.1029/2010JF001684.
Seminara, G., and M. Tubino (2001), Sand bars in tidal channels. Part 1: Free bars, *J. Fluid Mech.*, *440*, 49–74.
Shaw, J. B., and D. Mohrig (2014), The importance of erosion in distributary channel network growth, Wax Lake Delta, Louisiana, USA, *Geology*, *42*(1), 31–34.
Shaw, J. B., D. Mohrig, and S. K. Whitman (2013), The morphology and evolution of channels on the Wax Lake Delta, Louisiana, USA, *J. Geophys. Res. Earth Surf.*, *118*, 1562–1584, doi:10.1002/jgrf.20123.
Slingerland, R., and N. D. Smith (2004), River avulsion and their deposits, *Annu. Rev. Earth Planet. Sci.*, *32*, 257–285, doi:10.1146/annurev.earth.32.101802.120201.
Socolofsky, S. A., and G. H. Jirka (2004), Large-scale flow structures and stability in shallow flows, *J. Environ. Eng. Sci.*, *3*(5), 451–462.
Soulsby, R. L., L. Hamm, G. Klopman, D. Myrhaug, R. R. Simons, and G. P. Thomas (1993), Wave-current interaction within and outside the bottom boundary layer, *Coastal Eng.*, *21*, 41–69.
Syvitski, J. P. M., and Y. Saito (2007), Morphodynamics of deltas under the influence of humans, *Global Planet. Change*, *57*(3–4), 261–282.
Syvitski, J. P. M., C. J. Vörösmarty, A. J. Kettner, and P. Green (2005), Impact of humans on the flux of terrestrial sediment to the global coastal ocean, *Science*, *308*(5720), 376–380, doi:10.1126/science.1109454.
Syvitski, J. P. M., et al. (2009), Sinking deltas due to human activities, *Nat. Geosci.*, *2*, 681–686, doi:10.1038/ngeo629.
Syvitski, J. P., J. N. Smith, E. A. Calabrese, and B. P. Boudreau (1988), Basin sedimentation and the growth of prograding deltas, *J. Geophys. Res.*, *93*(C6), 6895–6908, doi:10.1029/JC093iC06p06895.
Syvitski, J. P., K. I. Skene, M. K. Nicholson, and M. D. Morehead (1998), Plume1.1: Deposition of sediment from a fluvial plume, *Comput. Geosci.*, *24*(2), 159–171.
Temmerman, S., T. Bouma, J. Van de Koppel, D. Van der Wal, M. De Vries, and P. Herman (2007), Vegetation causes channel erosion in a tidal landscape, *Geology*, *35*(7), 631.
Tennekes, H., and J. L. Lumley (1972), *A First Course in Turbulence*, 300 pp., MIT press, Cambridge Mass.
Törnqvist, T. E., D. J. Wallace, J. E. A. Storms, J. Wallinga, R. L. van Dam, M. Blaauw, M. S. Derksen, C. J. W. Klerks, C. Meijneken, and E. M. A. Snijders (2008), Mississippi Delta subsidence primarily caused by compaction of Holocene strata, *Nat. Geosci.*, *1*, 173–176, doi:10.1038/ngeo129.
van Eerdt, M. M. (1985), The influence of vegetation on erosion and accretion in salt marshes of the Oosterschelde, The Netherlands, *Vegetatio*, *62*(1–3), 367–373.
van Prooijen, B. C., and W. S. Uijttewaal (2002), A linear approach for the evolution of coherent structures in shallow mixing layers, *Phys. Fluids*, *14*(12), 4105–4114.
Wang, F. C. (1985), Report 7: Analytical analysis of the development of the Achafalaya River Delta, 117 pp., US Army Corps of Engineers, The Atchafalaya River Delta, New Orleans, La.
Welder, F. A. (1959), Processes of deltaic sedimentation in the lower Mississippi River, *Tech. Rep. 12*, 90 p., Coastal Stud. Inst., La. State Univ., Baton Rouge.
Wright, L. D. (1977), Sediment transport and deposition at river mouths: A synthesis, *Geol. Soc. Am. Bull.*, *88*(6), 857–868.
Wright, L. D., and J. M. Coleman (1971), Effluent expansion and interfacial mixing in the presence of a salt wedge, Mississippi River delta, *J. Geophys. Res.*, *76*(36), 8649–8661, doi:10.1029/JC076i036p08649.
Wright, L. D., and J. M. Coleman (1974), Mississippi River mouth processes: Effluent dynamics and morphologic development, *J. Geol.*, *82*, 751–778.
Wright, L. D., and C. T. Friedrichs (2006), Gravity-driven sediment transport on continental shelves: A status report, *Cont. Shelf Res.*, *26*(17), 2092–2107.
Wright, L. D., J. M. Coleman, and M. W. Erickson (1974), Analysis of major river systems and their deltas: Morphologic and process comparisons, *Tech. Rep. TR-156*, Coastal Stud. Inst., La. State Univ., Baton Rouge.
Zolezzi, G., R. Luchi, and M. Tubino (2012), Modeling morphodynamic processes in meandering rivers with spatial width variations, *Rev. Geophys.*, *50*, RG4005, doi:10.1029/2012RG000392.